Department of Mechanical and Aerospace Engineering

Tool development for the estimation of production losses due to identified failure cases in large scale symmetrical PV systems with string inverters

Author: Elise Johanna Raja

Supervisor: Mr Graeme Hamilton Flett

Mr Maido Märss

A thesis submitted in partial fulfilment for the requirement of the degree
Master of Science
Sustainable Engineering: Renewable Energy Systems and the Environment

2019

Copyright Declaration

This thesis is the result of the author's original research. It has been composed by the author and has not been previously submitted for examination which has led to the award of a degree.

The copyright of this thesis belongs to the author under the terms of the United Kingdom Copyright Acts as qualified by University of Strathclyde Regulation 3.50. Due acknowledgement must always be made of the use of any material contained in, or derived from, this thesis.

Signed: Elise Johanna Raja   Date: 22.08.2019

Abstract

Operation and maintenance of solar photovoltaic parks in Estonia is rapidly growing field, in 2018 around 91% of existing capacity was constructed and connected to the electricity grid. Significant increase in solar electricity capability was encouraged by the government funded subsidies. Need for maintenance in case of failures comes hand in hand with new renewable solar capacity. Large scale photovoltaic parks are often closely monitored, and maintenance activities are carried out depending on the failures occurring. There are several ways for approaching maintenance and repair scheduling, the aim of this work is to provide decision support tool for taking into account financial factors. The idea is to evaluate lost production during the estimated failure period and indicate whether alternative more expensive but faster repair is justified.

Dissertation starts with the overview of failures and maintenance practices to provide theoretical background for understanding the mechanisms of power losses in the solar photovoltaic parks. Subsequently Excel tool is developed, and overview of the logic given in the corresponding paragraph. Tool is used for determining preferred actions in three failure cases on different levels and during the highest and lowest solar resources. In addition to tool advantages and possible implementation, its limitations and further work is addressed to offer critical review of the developed tool.

Main value arising from the dissertation is completed Excel based tool allowing faster hourly estimation of production losses, taking into account inserted park layout, failure type and weather conditions. It was concluded that financial justification is dependent on all parameters and developed tool proves to be able to aid with related issues. What is more, given dissertation gathers information about most common failures occurring in solar photovoltaic parks, accompanied by most common maintenance practices and self-generated graph illustrating interactions between photovoltaic panel failures.

Acknowledgements

Table of Contents

List of Figures

List of Tables

List of Abbreviations

AC	alternating current
CBM	condition-based maintenance
CCD	charged coupled device
DC	direct current
DHI	diffuse horizontal irradiance
EL	electroluminescence
EVA	ethylene vinyl acetate
GFI	ground fault interrupter
GHI	global horizontal irradiance
I-V	current – voltage
IGBT	insulated-gate bipolar transistor
IR	infrared
JB	junction box
LNG	liquified natural gas
O&M	operation and maintenance
PID	potential induced degradation
PM	predictive maintenance
PV	photovoltaic
UV	ultraviolet
VBA	visual basics for applications

1. Introduction

1.1. Overview and Challenge Identification

In the last decade solar photovoltaic (PV) panels have reached the stage where they are commonly used for electricity generation in both smaller as well as larger scale. In case of a medium and large scale PV parks, electricity yield is closely monitored, and maintenance carried out regularly. In case of a failure in operational solar PV park, it is important to decide when to schedule repairments. Commonly, if solar park owners are not active in the field of operation and maintenance (O&M), service is purchased from competent company.

With regards to Estonian market, operation and maintenance of solar parks is rapidly growing field. At the beginning of 2019, the total capacity of solar power plants was approximately 110 MW as reported by the transmission system operator Elering (Elering, 2019). It is worth mentioning that around 100 MW additional solar power capacity of total 110 MW was brought online during the 2018 (Petrova, 2019). This was mainly due to government funded support plans that ended with the last day of 2018. Thus, demand for O&M can be expected to increase.

One of the owners of Estonia's biggest solar park complex raised an issue that there is a lack of practical decision-making tools, that help to make financially smart decisions, when failures occur in the park. Commonly, decision is based on the severity of failure type – in case of more severe failures, corrective or extraordinary maintenance can be carried out as soon as possible. When it comes to smaller failures or failures when the solar resource is not at maximum (winter months for example), repairing can also be postponed. This problem becomes apparent when park owners are responsible for the decision whether to pay extra for fast device transportation in case of failure, or whether to fix single solar panels in an array.

1.2. Aim and Objectives

Overall aim of this project is to create a decision support tool for planning and carrying out maintenance activities in case of failure in the PV park in order to make financially smart decisions. The goal of this dissertation is to provide a knowledge background and tool that would aid to answer questions like, whether a week shorter transportation period is worth substantial additional cost or is it reasonable to buy new device from less expensive retailer, who is not ready to deliver it in same time than other providers. Given tool is meant for the usage of owners of solar parks as well as for O&M companies.

Objectives of this work are achieved by investigating the most common failure types as well as maintenance practices and focusing on creating a decision support tool for deciding when to fix problems based on the estimated production that is lost due to the failure. It is important to understand the mechanisms behind failures, also their influence on photovoltaic panel production and tests carried out to discover them on the field. This research is provided to offer technical knowledge to the reader. Tool development is done by following that it can be used for different parks in different sizes, if available optional usage of weather forecasts to make predictions more accurate, and possibility to specify failures based on the influence it has on the power production.

1.3. Scope and Approach

Core of the project is to develop a tool, that can estimate production losses. Given tool is expected to be applicable with different parks, it is achieved through usage of multiple parameters and information about structure of the park accompanied by the modelled hourly production of actual park. Hence, developed tool can be used to aid with scheduling spare part ordering and maintenance. Implementation of a tool is carried out in a case study of 4.7 MW installed photovoltaic panel park in Pärnu, Estonia and different scenarios considered to draw conclusions.

The first section of the work gives an overview of relevant literature on most common failure types and operation and maintenance practices in solar photovoltaic panel parks.

This section is expected to give reader knowledge about failures that can occur in photovoltaic modules in respect to the changes in output power and mechanisms behind. It also covers the practices in O&M and explains the failure detection and determination procedures. Given part is important to understand why and how problems are occurring and what are the steps taken to detect and fix them in operational solar power parks.

The second section of the work focuses on developing a tool, that can be tailored for parks in different sizes, taking into account the structure and devices used. It also includes part where detected failure of different component levels can be inserted and corresponding production loss estimated. This section provides explanation on logic and equations used in the tool. It finishes with explanation of tool output data and description of which conclusions can be drawn based on this data.

The third part of the work focuses on case study using developed tool in 4.7 MW solar power park in Estonia. Since given PV plant consists of four parks for legal clarity, modelling is carried out for each park separately. Helioscope web-based tool is used for creating layout and determining annual hourly production losses. Then different failure scenarios are created and run to analyse how production can influence profitability of maintenance.

Last sections provide critical discussion regarding the results attained in case study and report limitations of the tool, address the future work and conclude main outputs of given project.

2. Failure Modes Regarding Photovoltaic Panel Parks

The main parts of photovoltaic panel parks are photovoltaic panels, inverters and transformers. Photovoltaic panels implement photovoltaic effect in solar cells, made of silicon or other semiconductor materials, to convert sunlight into electricity. Photovoltaic panels are able to generate and conduct direct current when exposed to the sunlight. Photovoltaic panels are connected in series to form strings and strings are connected to the inverters in parallel. Series connection is used to build up voltage and parallel connection is used to build up current, both values have to be compliant with the inverter specifications. Inverters are used for converting direct current coming from the PV panel strings to the alternating current. Alternating current is used for delivering electricity over long distances. In case of large scale solar parks, transformers are often used to higher the voltage of electricity generated. This is done in order to minimise transmission losses. In given sections main failures for each component, PV panels, inverters and transformers are given. This is accompanied by the failure rates of components in solar parks.

2.1. Photovoltaic Panel Construction

To start with, a brief overview of PV panel parts and their purpose is given. Solar cells are made of silicon wafers. Silicon is semiconductor material, and it is doped in certain way to form negative type (n-type) and positive type (p-type) silicon layers (Shapley, 2011). In negative type layer there are a few more electrons than in usual silicon and in positive layer there are a few less electrons. Those two layers are combined to form pn junction and energy from photons makes electrons to move between layers. Metals are conductors and therefore used to conduct electricity from the solar cells to the external circuitry. Metallisation of a cell consists of gridlines (also known as fingers) and busbars. Cells are connected in series with cell interconnect ribbons (also known as tabbing ribbons). In Figure 1 positions of gridlines, busbars, cell and string interconnect ribbons are shown.
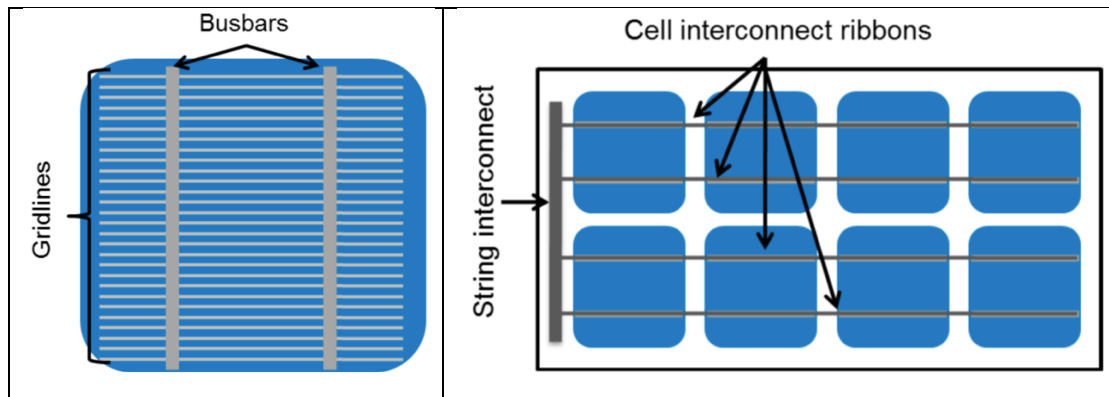
Figure 1. Illustration showing position of gridlines, busbars, cell and string

interconnect ribbons. Source (Köntges, et al., 2014)

Inspection of the busbars can be obscured by overlapping interconnect ribbons (Köntges, et al., 2014). Strings forming from cells connected in series with cell interconnect ribbons are connected with string interconnects.

Silicon cells are brittle and therefore have to be surrounded by layers that protect them from mechanical and thermal stresses. Encapsulant is used to bind together backsheet, solar cells connected with metallisation and upper layer glass. Those layers are also used to avoid moisture ingress that can cause corrosion, transparency changes and adhesion loss of encapsulant. In Figure 2 the construction of layers in solar panels is shown.
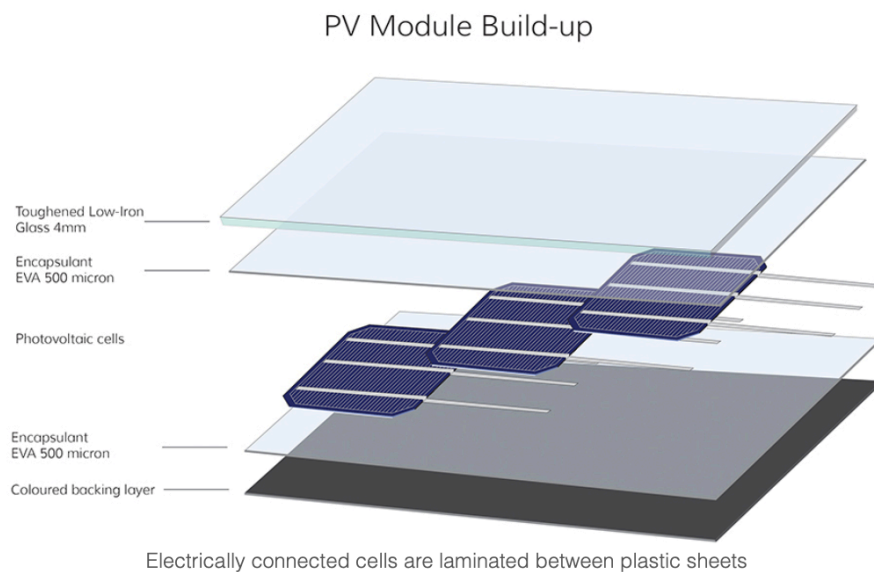
Figure 2. Illustration of solar panels construction. Source (Viridian Concepts Ltd.,

2017).

Layers of glass, encapsulant, cells and backsheet are surrounded by the frame, to provide means for fixing the panels to the roof or ground installations using clamps that are fastened to the frame.

Junction box is a container fixed on a backsheet of a solar panel containing bypass diodes. It has two wires direct current positive DC+ and direct current negative DC-, allowing PV panels to be connected to each other in series or in parallel (Power From Sunlight, 2017).
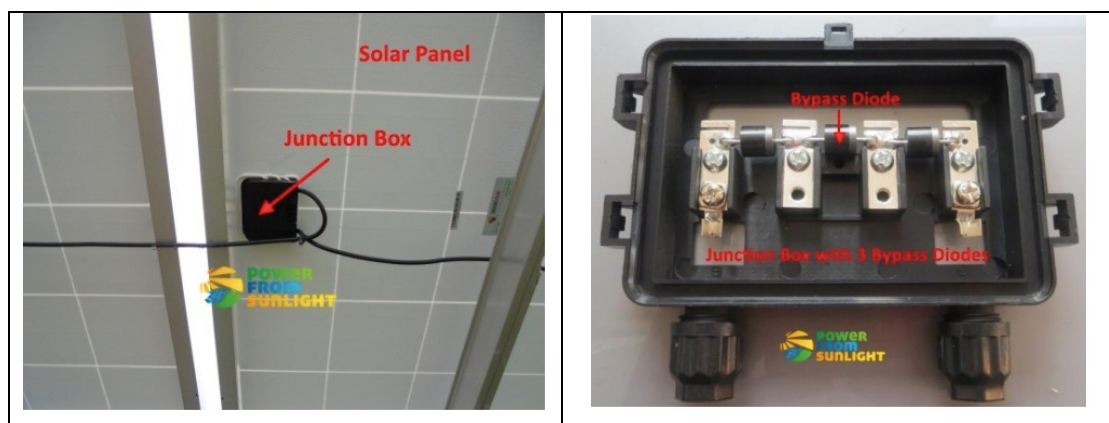
Figure 3. Pictures of junction boxes, on the left showing the location on the backsheet and on the right showing bypass diodes contained inside the junction box. Source (Power From Sunlight, 2017).

Bypass diodes minimise losses under partially shaded/soiled conditions and offer additional level of product safety in case of failures. Bypass diodes are connected to the cells in parallel and during normal operation are reverse biased (Power From Sunlight, 2017). If no power is produced by one or more solar cells, the current flows through the solar bypass diode and prevents hot spots and losses in yield (Power From Sunlight, 2017). A logic of turned on bypass diode is shown in Figure 4. Green arrows indicate the current flow. It can be observed that due to the shaded cell the middle bypass diode is turned on and is offering alternative path for the current to minimise losses and avoid further failures.
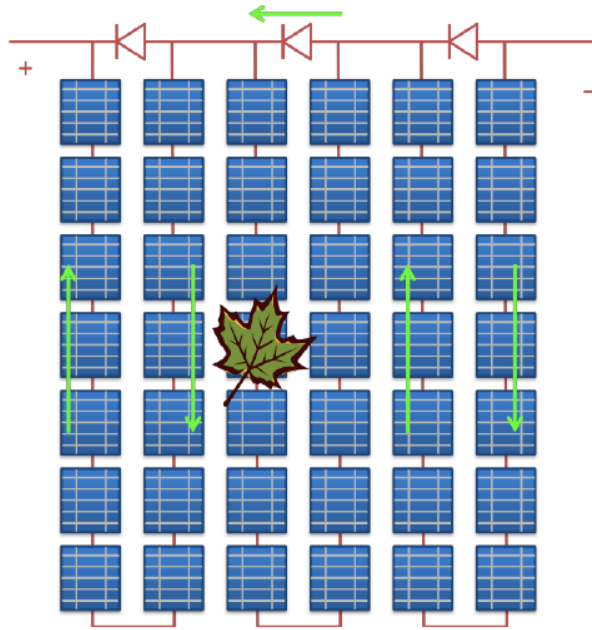
Figure 4. Illustration of a 42-cell module with 3 bypass diodes with the middle one being activated due to shaded cell in the corresponding string. Source (Klimaraad, 2018).

2.2. Failure Types of Photovoltaic Panels

The lifetime of a PV panel is mainly determined by the materials stability and resistance to corrosion (Honsberg & Bowden, 2019). The influence on the PV modules and their operation life can be separated into different failure and degradation modes. By definition, a PV module failure is an effect that degrades the module power which is not reversed by normal operation or creates a safety issue (Köntges, et al., 2014). Hence, not all causes that are responsible for the power output reductions, are failures. For instance, soiling or shading of the panel surface can be reversible and output power restored (Honsberg & Bowden, 2019). In addition, cosmetic failures that do not impose safety issue or degrade the module power, are not classified as failures (Köntges, et al., 2014).

Following sub-sections give an overview of most common wafer-based silicon module failures and degradation mechanisms, root of cause and possible influence on power output. Degradation mechanisms that are taken into account by the manufacturer (e.g.

light-induced degradation) and failures occurring due to errors in manufacturing or installation (e.g. improper mounting on the field) are not in the main focus of this work. In Table 1 summary of failures discussed in the following subchapters is given.

Failure	Affected area	Concerns	Expected losses
Delamination	Adhesion between solar panel layers.	Causes further degradation like corrosion, can result in electrical faults and panel failure.	Depends on the severity. Front side delamination obstructs the optical path, losses up to 4%.
Glass/frame breakage	Physical deformation of glass/frame.	Event causing it often deforms whole panel, or might weaken the panel. If not, it causes further degradation by allowing moisture ingress.	Depends on the severity, over time results in PV panel failure.
Junction box failure	Container, where bypass diodes are located.	Connections between modules can be affected. Bypass diodes can be affected.	Depends, which connections are affected. If modules connections are failed the whole string production can be lost.
Cell cracks	Solar cell silicon layer, that is responsible for the electricity generation.	Cracks in a silicon layer obstruct the path for electrons to form current, forming inactive areas that will not contribute to the energy generation and causing hot spots.	Depends on the severity. If more than 50% of cell is inactive, bypass diode is turned on and the string power inside module lost (in case of 3 bypass diodes, 1/3 of panel production is lost).

Encapsulant discolouration and	Encapsulant chemical composition and properties are changed.	Changes in properties can cause loss of adhesion between layers, water ingress, loss of transparency.	Mostly minor changes in power, unless the discolouration is severly localised in one cell, causing mismatch and/or bypass diodes to turn on.
Snail Trails	Silver paste used in the module production process.	Discolouration trails are formed. No significant further evolution is noted.	Does not cause losses, but indicates presence of cell cracks, that can be responsible for losses.
Hot spots	Temperature in cell increases.	High temperatures in cells can cause burn marks, cell cracks, delamination and discolouration.	Depends on the severity. Can cause bypass diodes to turn on. Severe delamination, burn marks require module change. Discolouration can result in permanent power degradation.
Potential Induced Degradation	Increased leakage currents towards ground.	Degradation effects are caused by the higher voltages and ion mobility.	Losses increase with increased voltage. Losses during low light conditions are proportionally higher.
Cell disconnection	Interconnect ribbon failure.	Cell disconnection can cause cell cracks, burn marks.	Measurements have shown that one interconnect ribbon failure can cause 35% and both interconnect ribbon failures 46% of losses.
Corrosion of metallisation	Metallisation responsible for the current flow is corroded.	Corrosion decreases conductivity of metallisation.	Depends on the severity.

Bypass diode failure	Bypass diode, being responsible for minimising losses by conducting current in case of mismatch.	Bypass diode failure in combination with mismatching can cause failure of the panel.	Bypass diode failure under normal conditions does not pose any losses. Bypass diode failure in case of mismatching in cell level can cause permanent failure of the panel.

Table 1. Summary table of most common wafer-based silicon module failures.

An easy-to-follow overview of failures and their interactions is given in Figure 5. It reflects the most common failure and degradation paths and is simplified in order to offer better understanding. Most of the impacts are reflected in the following subsections. For instance, moisture ingress promotes corrosion and encapsulant discolouration & delamination. Most commonly, moisture ingress is the result of glass or frame breakage. However, moisture ingress can be also a result of junction box failure or open burn marks, these reasons are neglected due to being less likely to occur. Therefore, given scheme can be used for understanding most common interactions, but is not meant for mapping all possible failure paths.
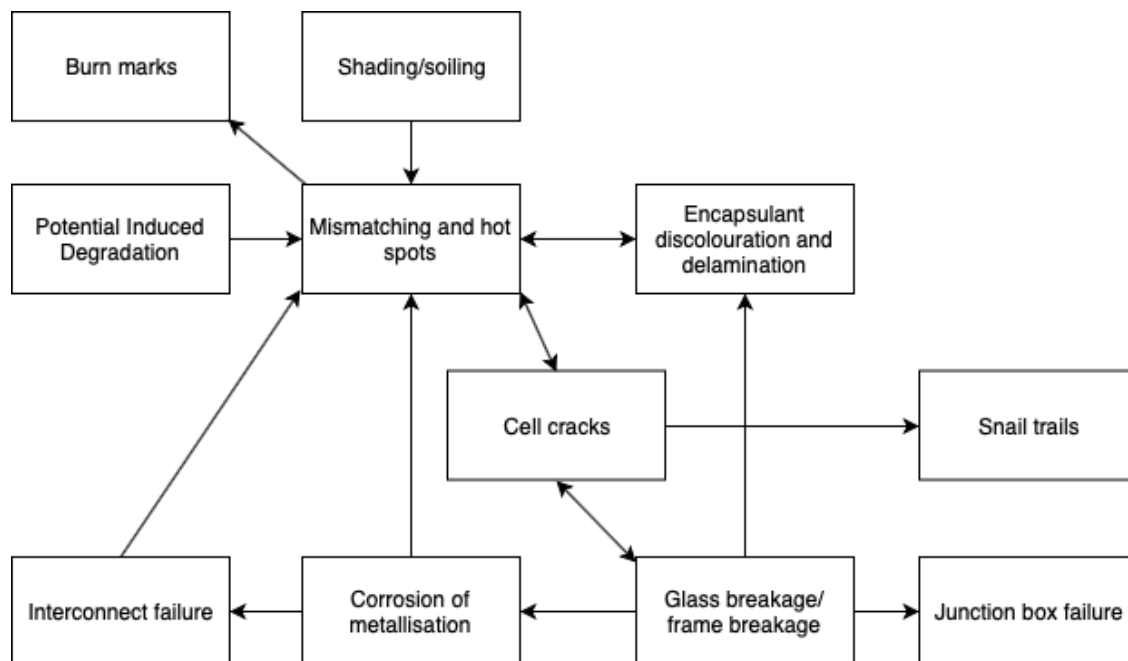
Figure 5. Failure interactions based on the literature review.

2.2.1. Delamination

Delamination is the compromised adhesion between glass, encapsulant, active layers, and back layers (Köntges, et al., 2014). Encapsulant is responsible for providing adhesion. The most common encapsulant used in PV panels is ethylene vinyl acetate (Badiee, et al., 2016). In order to offer better adhesion, encapsulant is usually formed with coupling agents that enhance adhesion, however such adhesive bonds can easily be decomposed by the small amounts of moisture penetrating from the edges of PV panel (Omazic, et al., 2019). Following delamination can lead to further moisture ingress and thus corrosion and changed pathways for electricity. In some cases delamination can enable exposure to active electrical components, result in an isolation fault, lead to a possibility of arcing etc., all posing safety issues (Köntges, et al., 2014). If the delamination occurs at the interfaces within the optical path, it is found that optical reflection can result in up to 4% of power loss at a single air/polymer interface (Köntges, et al., 2014).
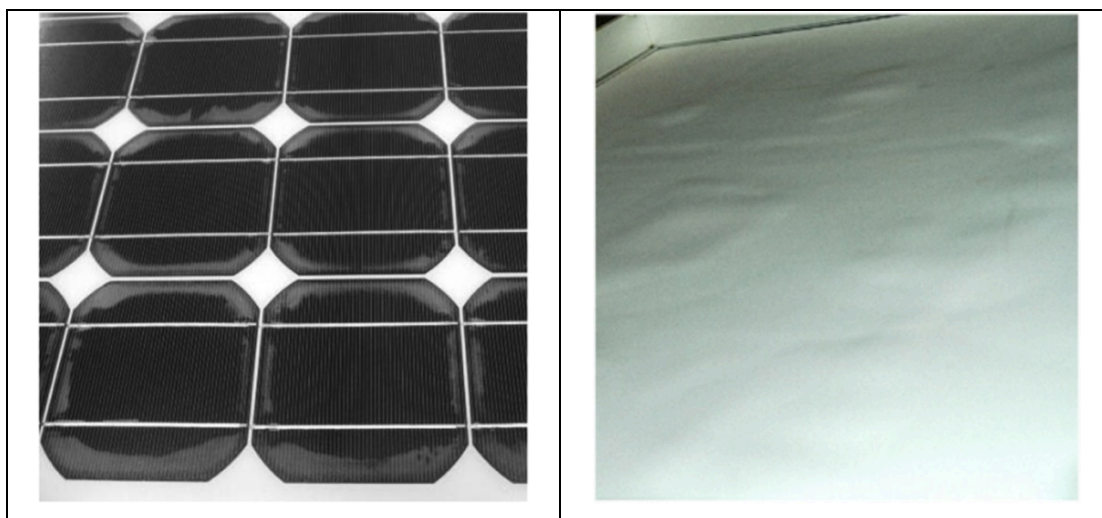
Figure 6. Delamination of the front encapsulant (on the left) and delamination occurring forming bubbles on the backsheet (on the right). Source (Omazic, et al., 2019)

Delamination can be apparent upon visual inspection as shown in Figure 6. Delamination can also occur between the encapsulant and backsheet. Most commonly backsheets have three layers, first being in contact with encapsulant has to offer durable adhesion and chemical compatibility with the encapsulant material, middle layer being thicker has to offer mechanical and electrical properties for the composite, and the outer

layer protecting from the environmental factors has to be highly reliable and stable (Omazic, et al., 2019). These layers are usually laminated together with adhesives (Omazic, et al., 2019). Formation of bubbles on the backsheet due to delamination does not have significant influence on the electricity generation. However, if delamination or bubbles occur near to the junction box or edges, it can result in a more severe failure (Köntges, et al., 2014).

2.2.2. Glass/Frame Breakage

The shattering of the glass or frame breakage can occur due to thermal or mechanical stress, e.g. heavy snow load or hail. Changes in the output power are dependent on the severity of damage. For instance, if solar cells do not get damaged, there might be no changes in the output power even when the glass is shattered. However, broken glass or frame allows moisture ingress, which causes corrosion. In different circumstances PV panel might get deformed and left inactive due to inflicted damage.

Figure 7. Image showing deformation of the panel due to mechanical forces. Picture taken in PV park used for the case study in Pärnu, Estonia.

Situation in Figure 7 is captured in non-operational solar park and given module has to be replaced before inverters are started in order to avoid further damage. Mechanical damage was inflicted during installation process.

2.2.3. Junction Box Failure

The connection of cell strings is located in the container named junction box (JB). It is fixed on the backside of the module and contains bypass diodes (Köntges, et al., 2014).

Figure 8. Images showing opened JB (on the left), poor fixing of the JB (in the middle) and bad wiring (on the right). Source (Köntges, et al., 2014).

There are several reasons for JB failure, namely poor fixing of the JB to the backsheet, opened or badly closed JB due to poor manufacturing process, moisture ingress which cause corrosion, and bad wiring causing internal arcing in the JB (Köntges, et al., 2014).

2.2.4.   Cell Cracks

Cell cracks are cracks in the silicon layer of the photovoltaic cells (Köntges, et al., 2014). Location, length and orientation of the crack determine whether it results in an open-circuited (inactive) cell part or gridlines and busbars allow the cell to continue functioning (Honsberg & Bowden, 2019) (Köntges, et al., 2014). Cell cracks parallel to busbars have the largest impact on the power performance (Gade, et al., 2015).

Cell cracks can appear during stages of silicon wafering, solar cell and module manufacturing, transportation and installation due to the brittleness of silicon (Gade, et al., 2015). They can also occur or lengthen after installation due to mechanical and thermal stresses. With an evolution of inactive area over 50%, power loss corresponds roughly to one third of the module power in case of solar module with 3 bypass diodes. It is due to the activated bypass diode that shortcuts 1/3 of the module (Köntges, et al., 2014). With the inactive cell area over 8% danger of hot spots emerges (Köntges, et al., 2014). Hence, the power loss depends on the type (length, location and direction) of the cell crack and can result in no detectable power loss as well as in inactive cell area, which influences the power and creates further degradation.
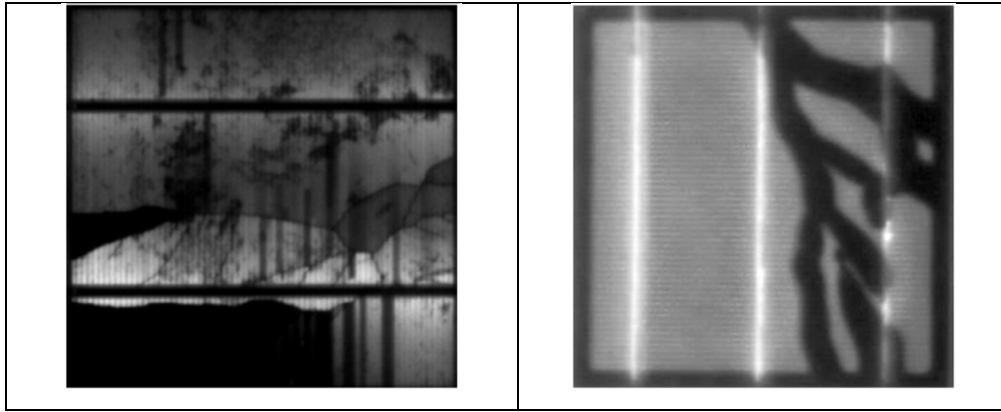
Figure 9. Electroluminescence (on the left) and ultraviolet fluorescence (on the right) images revealing cell cracks in different cells. Electroluminescence imaging reveals electrically disconnected areas. Source (Köntges, et al., 2014).

Cell cracks are not always apparent to the bare eye. They can be detected with electroluminescence and ultraviolet fluorescence imaging as shown in Figure 9. In field conditions, presence of snail trails is also an indication of the cell cracks.

2.2.5. Encapsulant Discolouration and Degradation

Encapsulant is used to electrically insulate Si cells and offer mechanical and thermal protection from environmental elements. Degradation of this layer can result in loss of power, loss of adhesion strength, delamination, and corrosion (Badiee, et al., 2016). Ethylene Vinyl Acetate (EVA) is copolymer of ethylene and vinyl acetate, and it is commonly used as encapsulant in the solar panels to bond silicon cell to the panel and backsheet due to the properties mentioned below. It has properties like high adhesion strength, high glass-like transparency, high electrical resistivity, a low polymerisation temperature and relatively low water absorption ratio in addition to low cost (Badiee, et al., 2016).
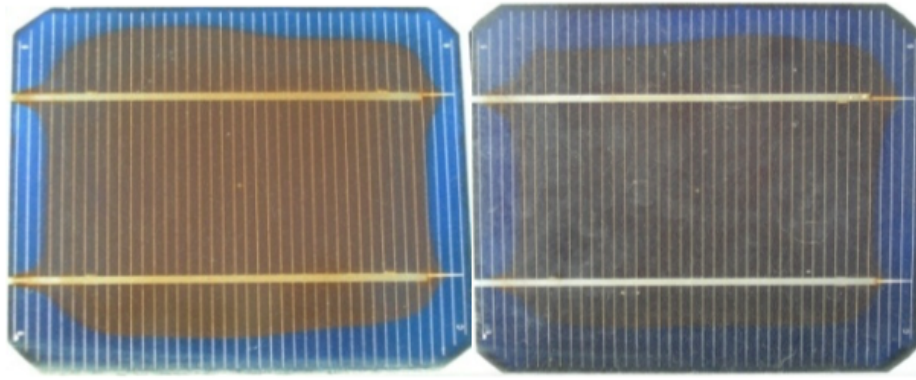
Figure 10. An example of EVA discolouration evolved in 18 years of operation. Source (Kaplani, 2012).

Discolouration is related to the combination of high temperatures, humidity and ultraviolet (UV) radiation that panels are exposed to in the field, causing chemical reactions in EVA layer. In addition to discolouration, exposure to field conditions can lead to changes in thermal and thermo-chemical properties leading to further degradation (Badiee, et al., 2016).

Commonly, discolouration can be determined during visual inspection before there is evident decrease in the module current and is mostly considered to be an aesthetic issue (Köntges, et al., 2014). However, EVA discolouration is expected to contribute to the overall degradation of the PV panels (Köntges, et al., 2014). Moreover, if discolouration is severe and localised at a single cell, it can trigger substring bypass-diode to turn on and therefore cause losses (Köntges, et al., 2014).

2.2.6.   Snail Trails/Tracks

Snail trails are grey or black discolouration tracks that form from silver paste used in the screen printing process where front screen contact structure is created (Köntges, et al., 2014) (Erath, 2009). Snail trails start to evolve after installation while being exposed to the field conditions. They are found to be occurring along cell cracks and edges of solar cells (Dolara, et al., 2016). After the first occurrence, snail trails have noted to have limited further evolution and no significant variation in terms of power losses (Dolara, et al., 2016).

The formation of snail trails is linked with used backsheet and encapsulant materials and their combination (Duerr, et al., 2016). For instance, encapsulant material plays a significant role for the formation of silver acetate and silver phosphate, both that are found in the snail trails of field failed PV modules (Duerr, et al., 2016). For prevention of snail trail occurrence, materials and their combinations have to be optimised (Duerr, et al., 2016).
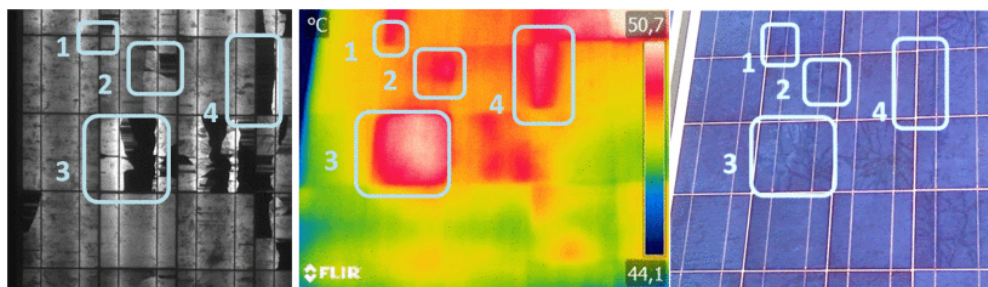
Figure 11. Electroluminescence (on the left), infrared (in the middle) and visual (on the right) images of the same PV module showing cracked cells, hot spots and snail trails on the same module, respectively. Source (Dolara, et al., 2016).

Snail trails are indicating the presence of cell cracks and are not responsible for their existence (Dolara, et al., 2016). Snail tracks are detectable upon visual inspection and electroluminescence imaging of the module reveals cracked cells. With infrared imaging it is possible to see hot spots caused by the cracked cells. Thus, the main power loss of modules showing snail trails comes from the cell cracks. However, modules affected by snail trails have a tendency of high leakage currents and can accelerate isolation of the cracked cell parts (Köntges, et al., 2014).

2.2.7. Hot Spots

Hot spots are PV module areas where temperatures rise to an extent where parts of the modules can be damaged. There can be several causes mainly due to cell failure, for instance like cracked cells, local shunts, mismatches, partial shadowing or failures in the interconnection between cells (Molenbroek, et al., 1991). Temperature increase causing overheating and hotspots can be prevented by limiting reverse voltage reaching

a shaded cell using bypass diodes (M.A.Munoz, et al., 2011). Presence of shunts that allow shortcut from one cell side to the other side or interconnection errors also resulting in shortcuts can generate hot spots (M.A.Munoz, et al., 2011). Mismatch between cells happens when one cell generates lower current than module string current, this results in higher operation temperature in given cell (M.A.Munoz, et al., 2011).
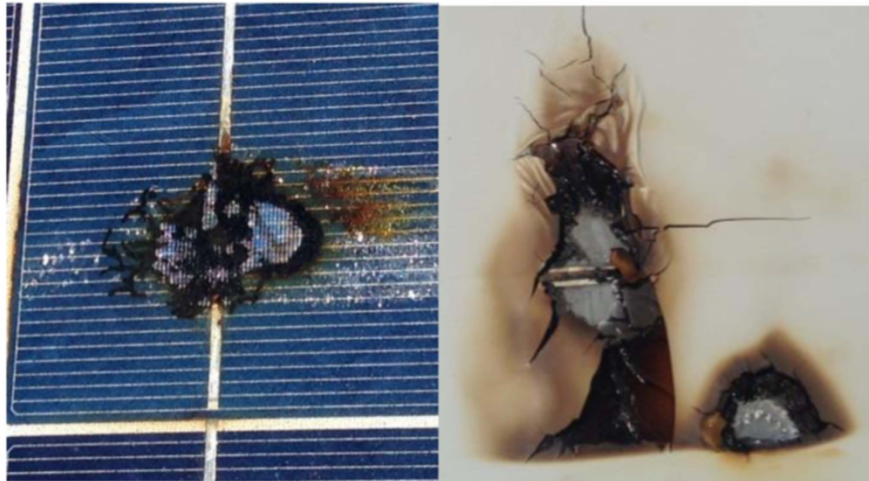
Figure 12. Image of the damaged module and backsheet, where hot spots reached over 300 ℃ resulting in burn marks. Source (Brooks, et al., 2015)

Hot spots can lead to burn marks on both front and/or back sides of the module. Hot spots can also cause cell cracks, EVA layer discolouration and delamination. Burn marks can evolve when the hot spot temperatures are increasing, and heat cannot be dissipated, or the root cause of hot spots eliminated.

Hot spots can be easily identified with thermography imaging as shown in Figure 13. Visual identification is possible after occurrence of burn marks and discolouration. Loss of current and therefore output power is dependent on the type of failure causing hot spots.
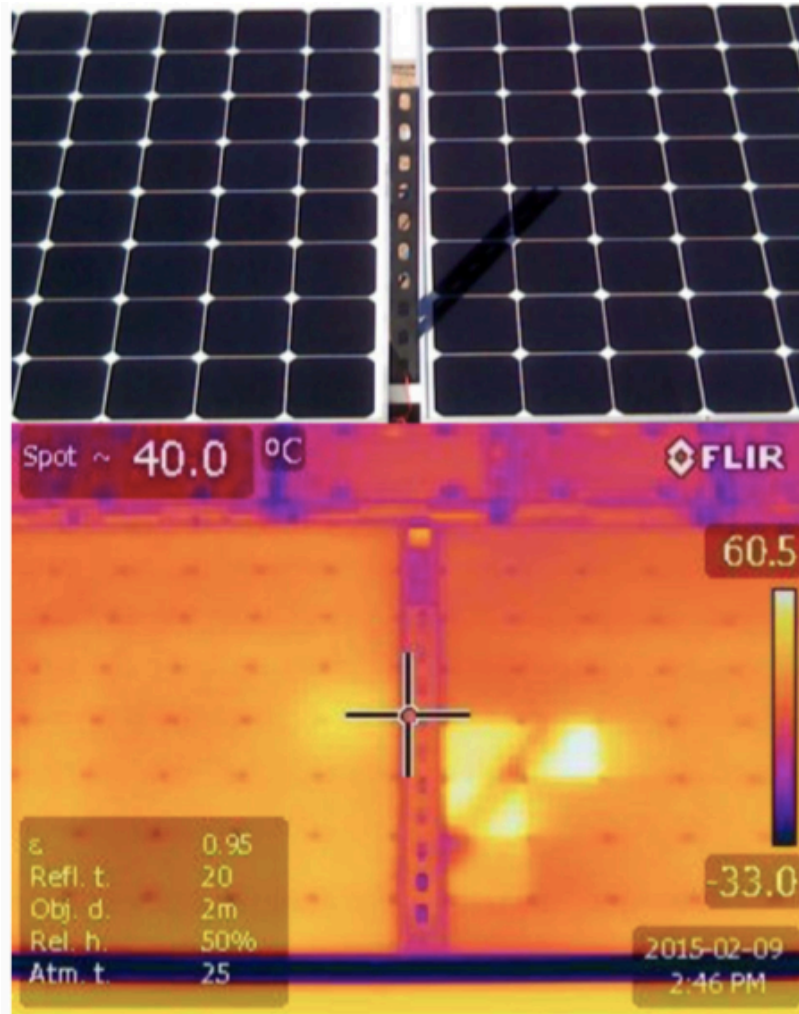
Figure 13. Visual (on top) and infrared (on bottom) image of the modules operating under partial shadowing causing hot spots. Source (Brooks, et al., 2015).

2.2.8. Potential Induced Degradation

Potential induced degradation (PID) is triggered by the high voltage and leakage currents in PV systems. With the increase in the share of electricity production from solar resources, sizes of parks and number of serially connected PV modules is increased. This, in return, determines higher relative potentials towards ground, which can cause ion mobility and leakage currents that are responsible for the degradation effects (Bauer, et al., 2012) (Pingel, et al., 2010). PID effects are dependent on the polarity and magnitude of applied voltage (Luo, et al., 2017). PID consequences become more severe with the increasing voltages (Köntges, et al., 2014). Several factors are found to contribute to PID effects, namely properties of antireflection coating,

encapsulation materials, presence of frame, temperature, humidity, grounding of the glass and solar irradiation conditions (Luo, et al., 2017).

The most common form of PID in p-type crystalline silicon-based modules is PID-shunting (Luo, et al., 2017). It has been shown that reduction of the shunt resistance and increase of the dark saturation current and Na ion mobility is associated with this type of PID (Luo, et al., 2017). It was discovered that defects in atom level structure i.e. stacking faults in Si were contaminated with Na, degrading electronic properties of solar cells (Luo, et al., 2017). Reduction of parallel resistance i.e. presence of shunt resistance allows current to flow in alternate paths and not through cell junction, causing losses (Honsberg & Bowden, 2019). During low light conditions losses become especially apparent since there is less available light and losses are proportionally larger (Honsberg & Bowden, 2019). This type of PID can be reversible with thermal and reverse-biased voltage recovery (Lausch, et al., 2014).

In n-type modules surface polarization is driven by high positive potential, which causes leakage current to flow through the panel to grounded frame and cause negative charges to accumulate on the antireflection coating (Luo, et al., 2017). As a result light-generated positively-charged holes are more attracted to antireflection coating that to p-n junction of the cell, this increases current and voltage (Luo, et al., 2017). As mentioned above, mismatch is caused when one cell generates lower current than others. Mismatch lowers efficiency of the panel and can cause hot spots and further damage.
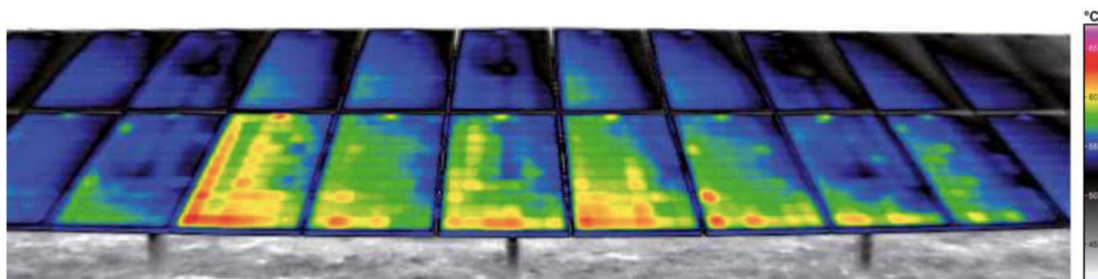
Figure 14. Infrared image showing heating in the shunted areas caused by the negative module voltage decrease from right to the left. Source (Köntges, et al., 2014).

In field conditions infrared imaging is suitable for the PID detection. PID prevention can be done in system, panel and cell levels. Usage of micro-inverters lowers the number of panels connected in series and therefore lowers relative potential towards ground. In case of p-type of c-Si modules it is important to make sure that active circuit of PV modules is not negatively biased relative to ground or that reversed voltage is applied during the night time (Luo, et al., 2017). Prevention methods in panel and cell level are associated with materials and manufacturing processes.

2.2.9. Cell Disconnection Due to Ribbon Failure

Interconnect ribbon is an electrical conductor attached to a PV module to connect the front side of the solar cells to the rear side. It enables electric current to flow by collecting light-generated electrons and holes to positively and negatively charged contacts, respectively (Ogbomo, et al., 2017). Process where electrons recombine with the holes before they can be conducted away as electric current is named recombination (Ogbomo, et al., 2017).
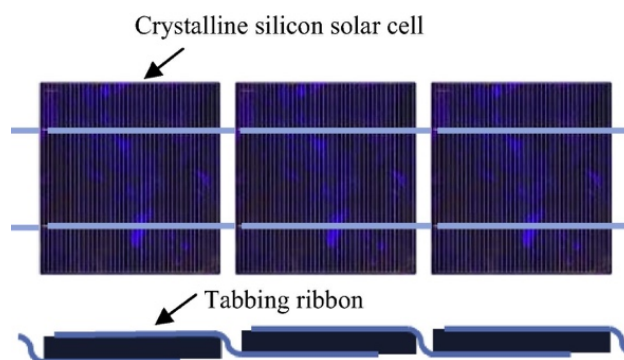
Figure 15. Illustration of interconnect/tabbing ribbon connecting the front and rear sides of c-Si solar cells. Source (Zarmai, et al., 2015).

Therefore, cells become disconnected if interconnect ribbon fails, causing heating and hot spots in disconnected cell. Interconnector failure occurs mainly due to mechanically weak ribbon kink or poor soldering of the connection between tabbing ribbon and string interconnect, and is triggered by physical or thermal stress like transportation or hot spots (Köntges, et al., 2014).
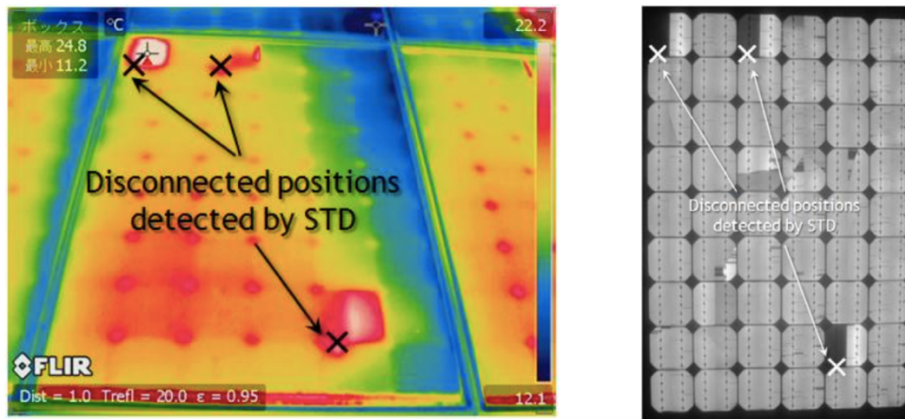
Figure 16. Infrared image (on the left) and electroluminescence image (on the right) of the disconnected cells in a PV module. Source (Köntges, et al., 2014).

Detection of the disconnected cells can be through infrared, electroluminescence and UV fluorescence imaging as well as with signal transmission device (STD). Based on the measurements introduced by (Köntges, et al., 2014) power loss of 35% appears with one disconnection and power loss of 46% appears with one cell failure due to both interconnection ribbons being disconnected, current flow is through bypass diode. If given bypass diode fails, it is followed by overall failure of the panel (Köntges, et al., 2014).

2.2.10. Corrosion and Discolouration of Metallisation

By definition, corrosion is the destructive attack of a metal by chemical or electrochemical reaction with its environment (Revie & Uhlig, 2008). Most of the metals tend to lose electrons to the substances in the environment (mainly oxygen), resulting in reduced oxygen that forms an oxide with the metal (Anon., 2019). Oxide layer, however, changes the electrochemical properties of the metal and therefore is responsible for the degradation of the PV modules. Corrosion can occur with the ingress of water vapor and oxygen, which is usually result of delamination or glass/frame breakage (Köntges, et al., 2014). Degradation of the EVA layer can also result in corrosion due to the formation of corrosive by-products like acetic acid (Badiee, et al., 2016). Hence, in the field conditions, corrosion often occurs in conjunction with EVA discolouration (Kaplani, 2012).
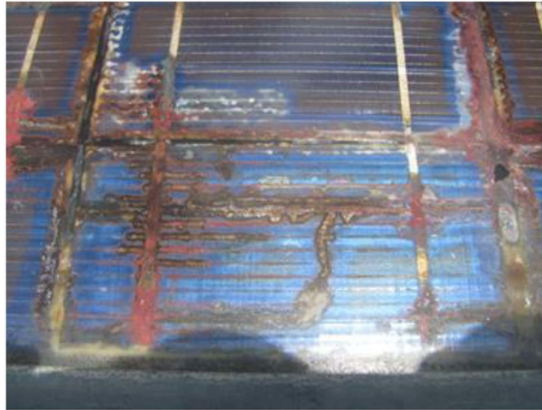
Figure 17. Severe corrosion of the metallization of the PV module. Source

(Wohlgemuth, et al., 2015)

Corrosion of metallisation is generally visible to the bare eye, especially in severe cases. The extent of power loss depends on the range and severity of corrosion. Increased high resistance in series resistance, due to the corrosion, can be observed in the current – voltage (I-V) curve as a slope (Kaplani, 2012).

2.2.11. Bypass Diode Failure

Bypass diodes are used for minimising losses in case of mismatching of cells. There can be several reasons for triggering bypass diodes to activate e.g. partial shadowing and cell cracks. Bypass diodes are connected in parallel to a small group of series connected cells, but with opposite polarity (Honsberg & Bowden, 2019). Under normal operation bypass diodes are open circuits due to their reverse bias (Honsberg & Bowden, 2019). However, in case of a mismatch in short circuit current between cells connected in series, mismatched cell becomes reverse biased and bypass diode allows the current of other cells to flow in the external circuit rather than forward biasing other cells in this series (Honsberg & Bowden, 2019). Bypass diodes used for PV modules are most often Schottky diodes, that have metal-semiconductor junctions and therefore lower threshold voltage and fast switching speed in order to allow quick operation of reverse voltage in case of short time (less than a minute long) shading occurs (Shin, et al., 2018).

Bypass diode failure can often be due to overheating or undersizing (Honsberg & Bowden, 2019). In a study conducted by (Shin, et al., 2018) overheating issue was monitored. It was found that thermal runaway, a process where high temperature in junction box causes leakage current of the bypass diode and this in return causes further increase in internal temperature, can cause failure of the bypass diodes (Shin, et al., 2018).

Bypass diode failure can result in permanent damage, if cell is subject to mismatch. In a study conducted by (Brooks, et al., 2015) it was found that the failure in case of bypass diode error and mismatch in cell is dependent on the reverse bias voltage of the cell. Module with high reverse bias voltage of -15 volts received permanent damage after one week of operation with partial shading. However, module with reverse bias voltage of -4 volts did not show any signs of damage or power loss from standard test conditions (Brooks, et al., 2015). Bypass diode failure will affect the production in case of mismatch between cells, this can happen due to shading, cell cracks, EVA discolouration etc. Based on the severity of mismatch and reverse bias voltage of the cell, PV module can be prone to total failure.
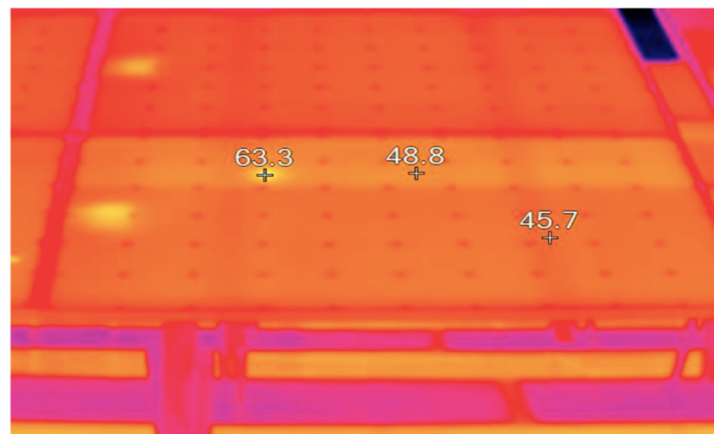
Figure 18. Infrared image of the PV panel with failed bypass diodes. Source (Shin, et al., 2018)

Bypass diode failure can be detected with infrared imaging, since failed bypass diode constitutes a closed circuit with the connected solar cell and increases local temperature (Shin, et al., 2018).

2.3.   Inverter and Transformer Failures

Solar inverters are used for converting direct current from photovoltaic panels to alternating current, to be forwarded to consumer or connected to the electrical grid. There are three main configurations for inverters, namely micro, string and central (Tariq, et al., 2018). Micro-inverters are usually connected to a single PV panel, while string and central inverters are connected to several panels. Micro-inverters are therefore optimizing power output from one panel, making it to work on the most effective current and voltage (Scholten, et al., 2013). As string and central inverters are connected to several panels, they have less flexibility and are not preferred in conditions like multi-angled roofing or arrays with significant shading conditions (Scholten, et al., 2013). However, string and central inverters are both used in large installations, where micro inverter implementation is not feasible.
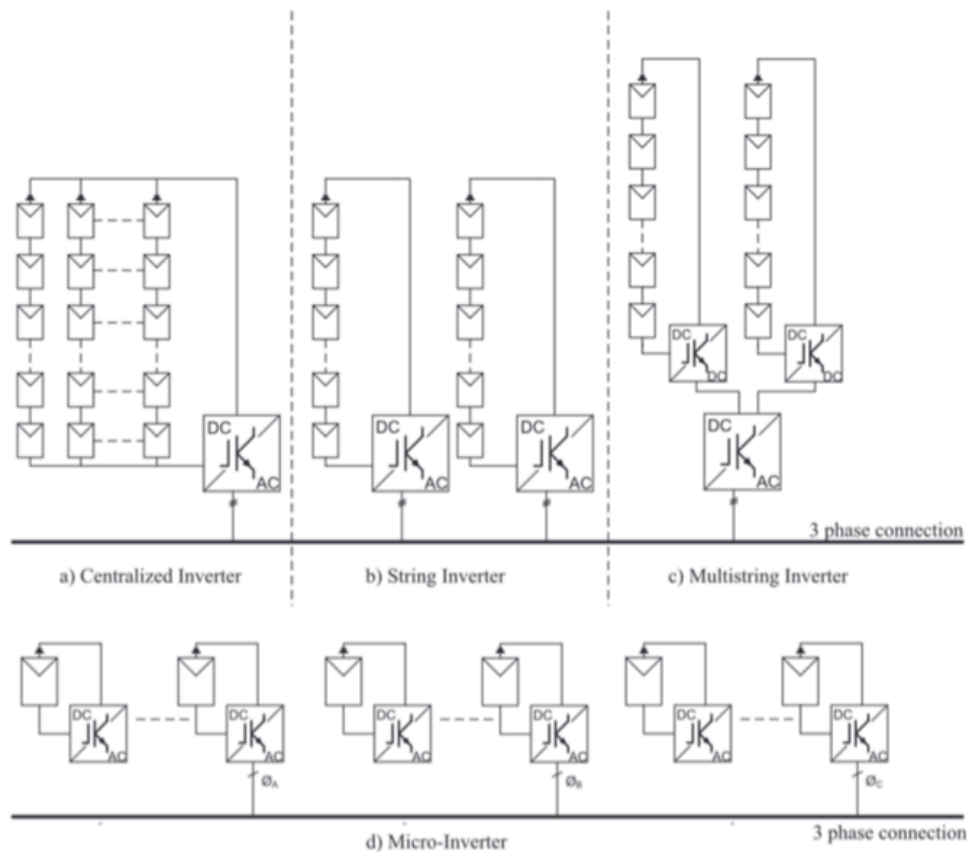
Figure 19. Configuration of central, string and micro-inverters. Source (Celik, et al., 2018)

There are several reasons for inverter failures that can be divided into failure areas as introduced by (Formica, et al., 2017), namely failures in card/board, alternating current (AC) contactor, fan(s), matrix/insulated-gate bipolar transistor (IGBT), power supply, AC fuses, direct current (DC) contactor, surge protection, ground fault interrupter (GFI) components, capacitors, internal fuses, internal relay/switch, DC input fuses. Those failures can be triggered by wide range of factors, for instance mechanical forces, incorrect sizing, heat accumulation, water and dust ingress, and overvoltage on AC side due to weak networks (C Gascoigne Ltd. , 2019).

Transformers are electrical devices, that allow transformation of voltage of AC supply, that is needed to connect PV park to electrical grid. Electrical grids use high voltages to minimise losses over long distances. As with all the other components, faults in transformers can occur in different parts and components due to mechanical, electrical or thermal stresses (Jan, et al., 2015). Most common failures listed by (Jan, et al., 2015) are gathered in Table 2.

Part	Purpose	Failure Reasons
Winding	Windings are used for electricity flow, drawing or delivering the power.	Winding failures commonly result in burn-out or breaking. Dielectric faults caused by insulation breakdown Thermal losses in copper wirings creating hotspots and thermal stresses Mechanical faults like distortion, loosening or displacement of the windings caused by improper repair, bad maintenance, corrosion, manufacturing deficiencies, vibration and mechanical movement.
Bushing	Bushes are used to insulate a high voltage electrical conductor to pass through an earth conductor.	Transformer vibrations can result in loosening of conductors and overheating. Given heat damages the insulating paper and the surrounding oil. High fault voltages cause partial discharge and bushes degeneration following by complete breakdown. Water ingress, aging or excessive dielectric losses cause seal breaking of bushes. This can lead to core failure. Internal over-flashing happens due to old oil or its deficiency.
Core	The function of a core is to concentrate the magnetic flux.	Cores are laminated in order to reduce eddy-current, that would otherwise cause thermal heating. Lamination can become defected due to poor maintenance, old oil or corrosion. Over-heating reaches the surfaces of the core that is in direct contact with windings, causing thermal damage. Given heat can also influence the oil to release gas and result in damage to other parts.

Tap changer	The function of a tap changer is to regulate the voltage level by adding or removing turns from the secondary wiring.	Run-through fault means that turn ratio is changed with delay. This can be caused by the residue flux (caused by polluted oil) remaining in the relay responsible for the tap change. Spring used for the tap change can also become fragile and cause this failure. Lack of maintenance can mean that shaft connection between the tap and the motor driver is not synchronous and tap changer can have the wrong position. Old capacitors or burned-out capacitor results in failed control of tap changer movement.
Tank	Tanks is used for storing oil in the transformer.	Tank wall cracks or leakage occurs due to environmental stress, corrosion, high humidity and UV radiation. The decreased oil levels result in reduction of insulation. Oil is also used for cooling and lower oil levels result in over-heating.
Protection system	Function is to protect the transformer from faults by detecting and resolving them.	Buchholz protection detects dielectric faults but can overheat and lose its sensitivity. Pressure relief valve circuitry protects from the overpressure from gas produced by overheated oil. Fault mainly occurs due to the fragile spring causing inability to reduce pressure. Failure also occurs in case of a rapid gas pressure increase since this system is only meant to release pressure slowly. Sudden Pressure Relays protect from sudden exponential increase of gas pressure to result in explosion. This relay can be affected by humidity and moisture in its internal circuitry. Surge protector protects transformer from over voltage by allowing specific magnitude of voltage, in case of failure high voltages pass to the windings resulting in further damage to the windings. Moisture, heat and corrosion are the main drivers for surge protector failure as they cause overheating and short circuit.
Cooling system	Function is to provide cooling of heat produced due to copper and iron losses.	Failure in the cooling systems causes heat to accumulate in the transformer causing further damage. Leak in the oil/water pipes causes reduction of fluids responsible for the heat exchange. Leakage can be triggered due to environmental stress, corrosion, high humidity and sun radiation. Fans used for the cooling can also fail, this is mainly due to poor maintenance, over use or motor wear-out. Faulty thermostats transmitting wrong temperatures cause cooling system to operate on wrong capacities.

Table 2. Table comprising failure data of transformers from (Jan, et al., 2015).

2.4.   Failure Rates of System Components

Previously collected field failure information is important to determine the failure rates of a specific components in a PV plant. It aids to estimate accurate energy losses and to schedule maintenance during the PV plant operation. In order to receive accurate analysis, it is important to include all the components contributing to the energy yield of the large scale PV systems. Failure rates given in this work are the same used by (Baschel, et al., 2018). They are chosen due to their detailed distribution of failures and given in the Table 3.

Component	Failure rate λ (failures per 10^6 hours)
PV module	0.035
PV connector	0.0056
PV string cable	0.002
String fuse	0.063
String monitoring unit	1.65
DC switch	0.2
DC main cable	0.0483
AC cable	0.013
Disconnector	0.1
String inverter	15.1
DC Capacitor	10.1
DC main breaker	6.075
Insulated-gate bipolar transistor (IGBT) module	11.4
AC filter capacitors	2
AC circuit breaker	6.075
Control and communication board	24.9
Cooling fan	27.4
Transformer	2.01
Power switch gear	4

Table 3. Failure rates of different components in large scale PV systems. Source

(Baschel, et al., 2018).

In addition to failure rates, it is important to take into account the repair and down-time of the components. As concluded in the work by (Baschel, et al., 2018), main contributors to the energy losses are transformer and inverter failures, even when their failure rates are very low compared to other components. It is due to the long replacement time for the devices like transformers and inverters. Hence, when it comes to analysis of a large scale PV plants, failure rates should be accompanied by the estimations for the time needed to repair problems and also the influence these components have for the whole energy yield. Energy yield during the specified failure can be calculated by using the tool developed in this project.

3. Maintenance of a PV Park and Failure Detection

Operation and maintenance (O&M) activities in a PV park aid to maintain the condition of a park and equipment in order to provide best production by avoiding losses due to failures and offering timely repair. According to the Best Practice Guidelines, maintenance of a PV plant can be divided into four categories based on the focus of the activities carried out, namely preventive, corrective, predictive and extraordinary maintenance (SolarPower Europe O&M Task Force, 2018). Alternative way to divide maintenance activities is to label them as preventative, corrective/reactive and condition-based maintenance (Enbar, et al., 2015). In addition to this, it is possible to identify maintenance based on the scheduling – scheduled or unscheduled (Solar DAO, 2017). There are several ways of how to categorise maintenance types and corresponding operations, but the main activities stay the same. It is decided to use division proposed by the Best Practice Guidelines and also refer to the similarities with other categories.

3.1. Preventive/Preventative Maintenance

Preventive maintenance is carried out intended to assess and/or to mitigate degradation and reduce the probability of failure of an item (British Standard, 2017). Preventive maintenance consists of regular visual and physical inspections (SolarPower Europe O&M Task Force, 2018). It also includes verification activities of all key components which are necessary to comply with the operating manuals and recommendations issued (SolarPower Europe O&M Task Force, 2018). This maintenance is carried out to prevent breakdowns and unnecessary production losses (Enbar, et al., 2015). All the activities carried out during the preventive maintenance should also comply with respective legal issues like national standards for periodic inspection of certain electrical components (SolarPower Europe O&M Task Force, 2018). Commonly, the periodicities or frequencies of inspections are agreed in the O&M contract and the contractor prepares the task plan until the end of the contract (SolarPower Europe O&M Task Force, 2018). Since it takes place on regular pre agreed intervals, it can be referred

to as a scheduled maintenance. Most common field inspections are infrared thermography, electroluminescence imaging and I-V curve tracking, and depending on O&M contract also often part of preventive maintenance.

3.1.1.　Infrared Thermography

Infrared (IR) thermography cameras measure thermal radiation of the inspected object and provide thermal image indicating temperatures using different colours. Since abnormalities in PV modules typically lead to higher electrical resistances and hence to a changes in temperature in affected area, those abnormalities in temperatures become evident during infrared imaging (SolarPower Europe O&M Task Force, 2018).

For high quality on-field images, inspections should be performed on a sunny cloudless day when solar irradiation is at least 600 W/m^2 and ambient conditions constant (Jahn, et al., 2018). Weather fluctuations must be slower than the time PV module takes to thermally stabilise for new ambient conditions like irradiation intensity, temperature and wind speed (Jahn, et al., 2018). Under uniform illumination and operation, cell temperatures may differ only a few degrees (Köntges, et al., 2014). However, temperature gradients occurring due to convective heat transfer must be accounted for (Köntges, et al., 2014). Overview of possible failures that can be detected with IR imaging are given in Table 4.

However, IR thermography alone is not always sufficient to reach a conclusive diagnosis and hence it is commonly combined with electroluminescence imaging and/or I-V curve tracking (SolarPower Europe O&M Task Force, 2018).
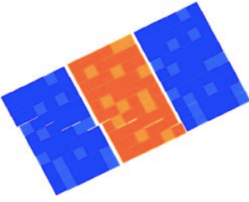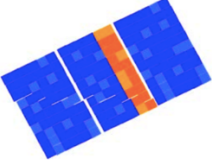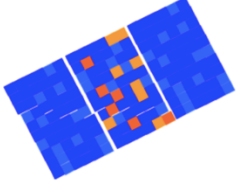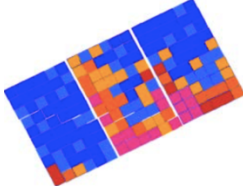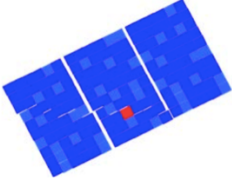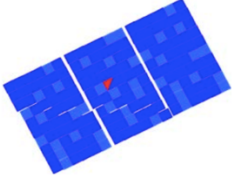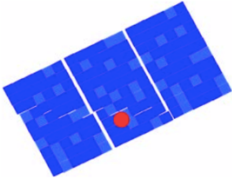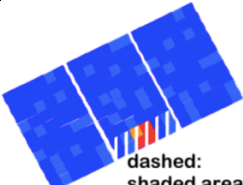
Pattern seen on IR image	Description and possible reasons
	If image indicates that one module is warmer than other modules, module is most likely open circuited and not connected to the system. This can be solved by checking the wiring and cables.
	If image indicates that one row (sub-string) is warmer than others. Bypass diode short circuit or internal short circuit can be possible reasons.
	If single cells are warmer and no pattern occurs, whole module is short circuited. This can be result of all bypass diodes being short circuited or due to wrong connection of module. Wiring and diodes have to be checked.
	If lower cells close to the frame are hotter than upper and middle cells, shunts are caused by the potential induced degradation and/or polarization.
	If one cell is clearly warmer than other cells, the failure is connected to this cell or surrounding conditions. Possible reasons include shadowing/local soiling, defect cell (cell cracks, corrosion etc) and delamination of cell.
	If part of a cell is warmer, possible reasons include cell cracks, burn marks and disconnected string interconnect.
	If there is pointed heating occurring on a module, possible reasons include shadowing/local soiling, cell cracks.
	If sub-string part is remarkably hotter than others in equally shaded conditions, it refers to bypass diode failure in given sub-string. Bypass diode failure with mismatching in cells can lead to panel failure.

Table 4. Patterns and failures that can be detected with IR imaging. Source (Köntges, et al., 2014).

3.1.2. Electroluminescence (EL) Imaging On-Site

Electroluminescence imaging represents detection of infrared radiation from the radiative recombination of PV modules (SolarPower Europe O&M Task Force, 2018). During the test PV module is supplied with a direct current (DC) from an external portable power source and imaging carried out with silicon charged coupled device (CCD) (Jahn, et al., 2018).

This procedure is usually done in a dark environment since the amount of near infrared radiation emitted by the PV modules is low compared to the radiation emitted by the background light (SolarPower Europe O&M Task Force, 2018). Thus, EL imaging in field conditions has to be carried out at sunset/during night or by using curtains supported by a frame to cover camera and module (Jahn, et al., 2018). A high pass edge filter may be used to reduce interfering light and improve imaging (SolarPower Europe O&M Task Force, 2018).

Electroluminescence imaging mainly aids with detecting cell cracks that can go unnoticed with infrared imaging, since not all cell cracks result in increase of temperature (Jahn, et al., 2018). In the EL image cell cracks appear as dark lines on the module (Köntges, et al., 2014). Overview of common failures that can be detected with EL imaging are given in Table 5.
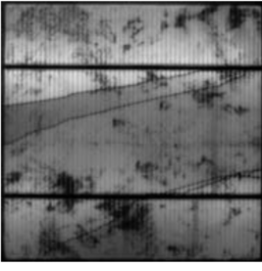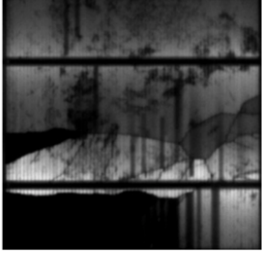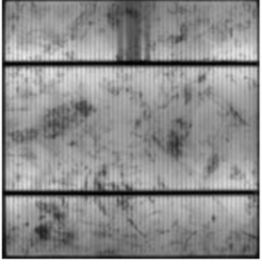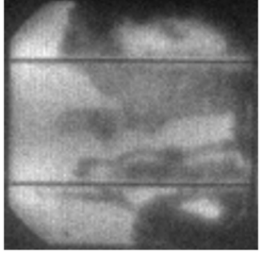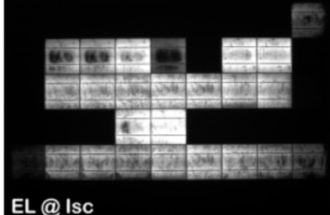
EL image	Description and possible reasons
	EL image indicates the presence of cell crack, but as seen from the image no inactive (disconnected cell parts are seen as black on EL imaging) cell parts are apparent. Therefore, given cell crack does not influence the current flow.
	EL image indicates the presence of cell cracks but compared to above picture clearly inactive areas can be seen on the lower left corner.
	EL image indicates gridline interruptions in the upper middle part caused by soldering.
	EL image indicates humidity corrosion on the right side of the cell developing towards middle and left part of the cell.
	EL image indication potential induced degradation (PID). It is possible to identify an early stage of PID before a power loss becomes apparent with EL images taken at 10% of short circuit current.

Table 5. Common failures that can be detected with EL imaging. Source (Köntges, et al., 2014).

3.1.3. I-V Curve Tracking On-Site

On-field measurements are carried out using portable I-V curve tracer, reference cell and thermometer (SolarPower Europe O&M Task Force, 2018). During the inspections, the current and voltage curve is measured while voltage across the module or current through the module is varied (Köntges, et al., 2014). I-V curve measurements can determine electrical parameters, namely maximum power (P_{mpp}), short-circuit current (I_{sc}), open-circuit voltage (V_{oc}), shunt resistance (R_{sh}) and series resistance (R_s) of single module or strings as shown in Figure 20 (SolarPower Europe O&M Task Force, 2018).
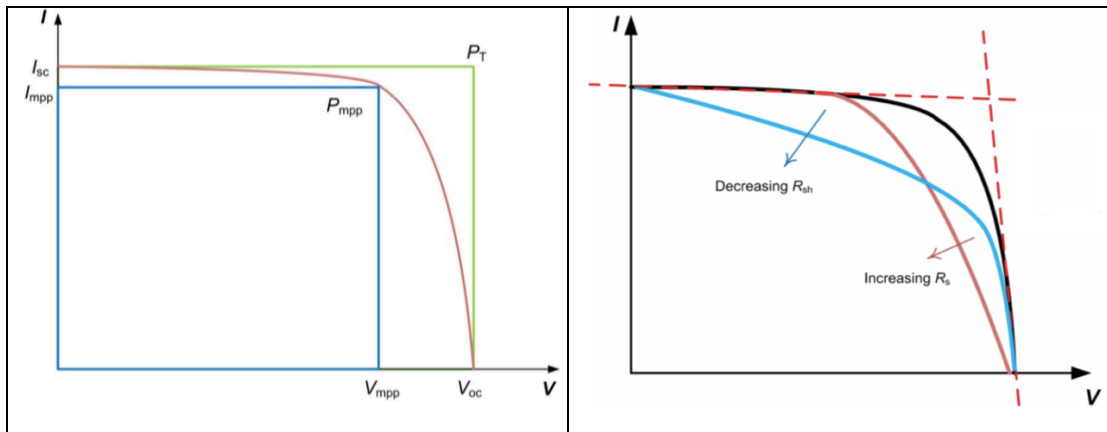
Figure 20. Illustration of an I-V curve. Source (Köntges, et al., 2014).

The maximum power (P_{mpp}) is a point on the I-V curve, where the product of current and voltage is maximal (Köntges, et al., 2014). Fill factor is the ratio comparing maximum power (P_{mpp}) to the virtual power (P_t) that would result if V_{mpp} would be the open-circuit voltage and I_{mpp} would be the short-circuit current (Köntges, et al., 2014). Shunt resistance (R_{sh}) illustrates a shunt path for the current flow bypassing the active solar cell and series resistance (R_s) shows all series resistances of the solar cells and interconnects together (Köntges, et al., 2014).Shape of the I-V curve helps to identify failures and overview of possible failures detectable from curve shape are given in Table 6 (SolarPower Europe O&M Task Force, 2018). In Table 6, current is on vertical and voltage on horizontal axis, green line indicates the curve without failure, red line indicates the curve with failure, and orange circle/line indicates the change.
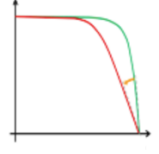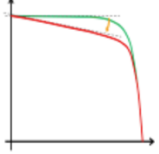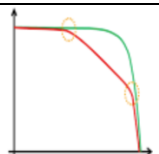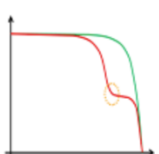
I-V curve shape	Description and possible reasons
	A lower short circuit current indicates that less irradiation reaches solar cells, it can be due to changes in transparency of encapsulation, glass corrosion, delamination or cracked cells.
	A lower open circuit voltage indicates that there can be failed cell interconnections, short circuits from cell to cell, failure of a bypass diode or potential induced degradation.
	Increase in the series resistance can be caused by increase of interconnections resistance, corrosion in junction box or interconnects and slacks joints.
	Decrease in the shunt resistance can be caused by shunts in the cells/interconnections, minor cell mismatch or non uniform transparency change of the AR coating, glass and encapsulant.
	Change in the slope can be caused by non uniform corrosion of antireflection coating and potential induced degradation.
	Steps forming in the I-V curve can be caused by the defective bypass diode, cell cracks, heavy mismatch of the cells, broken cell interconnect ribbons and non uniform changes in the transparency of the AR coating, glass and encapsulant.

Table 6. Overview of possible failures detectable from the I-V curve shape. Source

(Köntges, et al., 2014).

3.2. Corrective Maintenance

Corrective maintenance is carried out after the failure detection, with a goal to restore a PV plant system, equipment or component to a status where it can perform the required function (SolarPower Europe O&M Task Force, 2018). Failure detection can be done either by remote monitoring or during regular inspections carried out during preventive maintenance (SolarPower Europe O&M Task Force, 2018). Need for the corrective maintenance can be lessened through more proactive preventive and predictive maintenance (also known as condition-based maintenance) (Enbar, et al.,

2015). Generally, corrective maintenance can be broken down into troubleshooting the problem to identify the cause and localisation and then repair to restore the functionality (SolarPower Europe O&M Task Force, 2018). Temporary repair can be implemented when full repair has to wait for some reason, e.g. spare part has to be ordered and until it is received the old one is temporarily fixed.

3.3. Predictive and Condition-Based Maintenance

The British Standard EN13306:2017 Maintenance. Maintenance terminology differs between predictive maintenance (PM) and condition-based maintenance (CBM) by stating that CBM is preventive maintenance that includes assessment of physical conditions, analysis and the possible ensuing maintenance actions (British Standard, 2017). However, predictive maintenance is condition-based maintenance carried out following a forecast derived from repeated analysis or known characteristics and evaluation of the significant parameters of the degradation of the item (British Standard, 2017). This means that devices on site have to provide information about their state so O&M contractors are able to use real-time data to anticipate failures (Enbar, et al., 2015) (SolarPower Europe O&M Task Force, 2018). Technology to provide communication and monitoring software and hardware comes with the higher price tag, nonetheless it is found to increase overall efficiency of the park (Enbar, et al., 2015). By analysing data received it is possible to identify subtle trends that would otherwise be noticed only after next circuit testing or thermal imaging inspection (SolarPower Europe O&M Task Force, 2018). PM is found to anticipate maintenance activities, reduce time to repair, reduce spare parts replacement costs, reduce emergency and non-planned work, and improve predictability (SolarPower Europe O&M Task Force, 2018).

3.4. Extraordinary Maintenance

Extraordinary maintenance activities are needed when major unpredictable events take place and substantial works are required to restore previous condition of the PV plant (SolarPower Europe O&M Task Force, 2018). Such events include Force Majeure, theft, fire, serial defects on equipment occurring suddenly and months or years after

start-up, and regulatory changes requiring modifications (SolarPower Europe O&M Task Force, 2018). Due to its nature it is unscheduled and thus given activities are not included in corrective maintenance and are billed separately (SolarPower Europe O&M Task Force, 2018).

4. Estimation of a Production Losses Due to a Failure: Tool Development

Estimation of production losses is based on the two main components, firstly historical average weather data or weather forecast and created PV park model, and secondly detected failure and its range. While modelling, historical average weather data is commonly used, however, there is option to use custom weather data files. Weather forecast with created PV park model enables to forecast production specific for the PV plant and future weather conditions, while failure detection and its range determines the scale of the loss of production. It is up to the tool user to decide what kind of data and accuracy is needed. Based on data received from the tool, it is easier to make financial decisions, for instance when it is cost-effective to schedule maintenance. For given tool, it was important to keep it easy to implement but at the same time reasonably accurate. Therefore, it was decided that calculation of losses is based on the failure of components, not on the different failure types. Connection between failure types and component failures is given in Table 7.

Component Failure	Corresponding Failure Types
Bypass diode(s) activation due to a failure in solar cell(s)	Bypass diodes can be triggered on due to a mismatch in one or more cells in the string where bypass diode is connected to inside the module. It includes mismatching causing hot spots, cell disconnection, severe corrosion, cell cracks, and severe discolouration. Explanation of how bypass diodes work is given in subchapters 2.1 and 2.2.11.
PV panel(s) failure	PV panel failure occurs when the whole panel is unable to produce electricity. This can occur due to the all above mentioned failures, that are spread across the panel. This can also be due to the glass or frame breakage or severe delamination. Given tool allows to indicate several PV panel failures in one string.
Bypass diodes failure	Bypass diodes can fail due to an overheating, undersizing, junction box failure, thermal runaway in junction box, poor

accompanied by a failure in PV panel	wiring or soldering of contacts, delamination of a backsheet. In case of a PV panel failure that is accompanied by bypass diode(s) failure, the output changes accordingly to the number of failed bypass diodes.
Inverter failure	Inverter failures can be triggered by wide range of factors, for instance mechanical forces, incorrect sizing, heat accumulation, water and dust ingress, and overvoltage on AC side due to weak networks
Transformer failure	Transformer failures can occur in different parts and components due to mechanical, electrical or thermal stresses. Detailed overview is introduced in Table 2.
Grid connection failure	Grid connection failure indicates the situation where the whole park is unable to produce electricity. This can be due to technical reasons, but also for legal reasons regarding grid connection point etc.

Table 7. Connection between detailed failures described in theoretical part of this work and component failures used in the developed tool.

For instance, cell cracks can appear in different lengths, orientations and locations and also implement different production losses. However, if cell cracks trigger bypass diode(s) to turn on, it is relatively straight-forward to calculate the production loss as shown in subchapter 4.2.1. Smaller losses than the ones due to the bypass diode activation are neglected. It is due to the excessive information required and in many cases there is further research needed to accurately calculate losses due to the failure.

4.1. Weather Forecast and PV Plant Model

It must be noted that given tool can be used only in combination with model created based on specific PV parks. Estimated hourly production from the simulation tool is input for the tool developed in this project. There are several simulation and designing software on the market. For given tool, it does not matter what kind of software is used, as long as the output data is hourly and there is possibility to use custom weather data

files, if decided. Alternatively, default weather data for given location can be used, if there is no weather forecast available, the period exceeds couple of weeks, or user does not wish to use custom weather data. Most commonly, weather data needed includes global horizontal irradiance (GHI), diffuse horizontal irradiance (DHI), ambient temperature, and windspeed. As such models are based on the real PV plants, the modelling using HelioScope is described in the section 5.

4.2. Failure Impact and Production Loss Calculations

Failure detection and determination is vital in order to benefit from the tool. As shown in the literature review chapter, there are several failures that have different causes but similar outcome. For instance, bypass diode can be triggered to turn on due to disconnected cell or mismatch, which can be the result of soiling or severe discolouration of the encapsulant. Production loss due to bypass diode turning on is the same, even when the reason for that to do so is different. Therefore, it is important to understand the result of different failures. In this tool, production loss is calculated based on the information inserted in the table. Example of a table is given in the Figure 21. Data inserted about the park is corresponding to the park used in the case study. Failure of 3 panels in the same string is inserted.

Please note that information should be entered in the white squares, grey squares indicate that these values should not be changed			
Based on the PV plant layout fill in the following:	**Nr of units**		
Nr. of grid connection	1		
Nr. of transformers/AC combiners	1		
Nr. of inverters connected to one transformer/AC combiner	10		
Nr. of strings in one inverter	18		
Nr. of PV panels in one string	18		
Nr. of bypass diodes in one PV panel	3		
Whole PV plant specs	Nr of units		
Transformers	1		
Inverters	10		
PV panels	3240		
Based on the failure type fill in the following:	**OK/failed**	**nr of units affected**	**percentage working**
Grid connection	ok		0,999074074
Transformer/AC combiner	ok		0,999074074
Inverter failure	ok		0,999074074
Bypass diode(s) failure (accompanied by failure in PV panel)	ok		1
PV panel failure	failed	3	0,833333333
Bypass diode(s) turned on			1

Figure 21. Table introduced in the tool for the calculation of production losses

As seen from the Figure 21 it is expected that person using the tool has data about the failure and its range. Failures are divided into 6 stages indicating different failure scales. The larges impact is in case of grid connection failure, where the whole solar park can be offline. Transformer and inverter failures impact the production coming from the connected devices and modules. The factor at which the solar park is working at is calculated based on the information inserted about the total number of devices and number of failed devices.

Lower level failures include the PV panel and series connected PV panels called strings. There are three possible failure combinations:

1) failure in one or more of the cells that are connected in series in module and connected to the bypass diodes, due to the failure one or more bypass diodes are turned on and the production of PV panel decreases respectively to the number of bypass diodes used in the panel. Commonly 3 bypass diodes are used in single module. In case of one activated bypass diode 1/3 of the production is lost;

2) failure in PV panel, where it is unable to produce electricity, but is able to conduct it so string power is only reduced by the panel power that is failed;

3) failure in a PV panel is accompanied by bypass diode failure, depending on the number of bypass diodes failed string power is calculated.

All of the factor calculations described are introduced in detail in subchapters 4.2.1, 4.2.2 and 4.2.3. It must be also noted that if there is failure in PV panel level as shown in Figure 21, the percentage of functional park is calculated in string level (corresponding to 83%) and in output level from inverters (corresponding to 99,9%). If there would be several transformers and grid connections the calculation would continue. Final factor is used to calculate production losses.

4.2.1. PV Module Power

Under ideal conditions PV module power differs from the nominal power due to failures and degradation. In most cases severe failure triggers a bypass diode to turn on. There are several reasons why bypass diode(s) can be activated, for instance mismatching between cells connected in series in the module. However, once the bypass diode is

turned on, the reason behind it is neglected and losses are dependent on the number of bypass diodes implemented in the module. Cells that are in a series with turned on bypass diode will not conduct electricity. Therefore, the efficiency of the PV panel is

$$F_{PV\ module} = \frac{N_{bypass\ diodes} - N_{activated}}{N_{bypass\ diodes}} \tag{1}$$

where,

$F_{PV\ module}$ = a factor of panel output power;

$N_{bypass\ diodes}$ = a number of bypass diodes in given panel type;

$N_{activated}$ = a number of bypass diodes that are activated in given module.

If the failure in PV panel is followed by the bypass diode failure, the panel output is calculated likewise, difference is in the string power calculation.

4.2.2. PV Panel String Power

In a PV park panels are commonly connected in series forming strings to build up voltage and connected to inverters in parallel to build up current. Therefore, one string consists of a number of series connected PV panels. If there is failure in a PV panel and it is not able to produce electricity, but is able to conduct electricity, the output from this string is

$$F_{string} = \frac{N_{modules} - N_{failure}}{N_{modules}} \tag{2}$$

where,

F_{string} = a factor of string output power;

$N_{modules}$ = a number of PV modules in given string;

$N_{failure}$ = a number of PV modules that have failed in given string.

In case of an activated bypass diode(s) calculation of string output is

$$F_{string} = \frac{(N_{modules} - 1) + F_{PV\ module}}{N_{modules}} \tag{3}$$

where,

F_{string} = a factor of string output power;

$F_{PV\ module}$ = a factor of panel output power with activated bypass diode(s);

$N_{modules}$ = a number of PV modules in given string.

However, when PV panel has failed and it is followed by the bypass diode(s) failure, given PV panel is not able to (fully) conduct electricity. In this case the string output is

$$F_{string} = F_{PV\ module} \tag{4}$$

where,

F_{string} = a factor of string output power;

$F_{PV\ module}$ = a factor of PV module output power in case of the failure.

4.2.3. Output Power from Inverters, AC Combiners and Transformers

Large scale PV parks use multiple inverters to accommodate electricity conversion from DC to AC. In case of an inverter(s) failure(s), output power from inverters is calculated using equation likewise to (2)

$$F_{inverters} = \frac{N_{inverters} - N_{failure}}{N_{inverters}} \tag{5}$$

where,

$F_{inverter}$ = a factor of inverters output power;

$N_{inverters}$ = a number of inverters connected to the AC combiner or transformer;

$N_{failure}$ = a number of inverters that have failed.

If the failure lies in the lower level device, e.g. string level, the output from inverters is calculated as follows

$$F_{inverters} = \frac{(N_{inverters} - 1) + \frac{(N_{strings} - 1) + F_{string}}{N_{strings}}}{N_{inverters}} \tag{6}$$

where,

$F_{inverters}$ = a total factor of output power from inverters;

F_{string} = a factor of string output power in case of a failure in one of its PV panels;

$N_{inverters}$ = a number of inverters connected to AC combiner or transformer.

$N_{strings}$ = a number of strings connected to one inverter.

Large scale PV parks commonly use AC combiners to combine cables from different inverters before transformers. Transformers are devices used to minimise electricity transmission losses by reducing the current and increasing the voltage. AC Combiner and transformer output power calculations are straightforward, following the logic used in equations (2) and (5). If the failure lies in the lower level device, e.g. inverter level, the calculation takes into account relevant factor and follows the logic used in equation (3).

4.2.4. Production Losses Calculation

Tool is able to calculate the factor that PV plant is working at, based on the information provided about failures. Given factor is used to calculate production losses from the production data inserted. Small Visual Basic for Applications (VBA) script in Excel was written in order to receive production losses from the period specified. Since the tool is used for the Estonian market financial calculations use relevant price information. Hourly data from Nord Pool about electricity prices in 2018 is used. Additional marginal can be added to the market prices. However, if calculations require other markets, different price data can easily be inserted in relevant column.

4.2.5. Worked Example of Calculations Implemented

In Figure 22 exemplary situation is introduced. It can be seen that given park complex consists of 1620 PV panels, 30 inverters and 6 transformers. One inverter has 6 strings each formed from 9 PV panels connected in series. 5 inverters are connected to each transformer. 3 transformers are connected to each grid connection point and in total there are two grid connection points.

Please note that information should be entered in the white squares, grey squares indicate that these values should not be changed			
Based on the PV plant layout fill in the following:	Nr of units		
Nr. of grid connection	2		
Nr. of transformers/AC combiners	3		
Nr. of inverters connected to one transformer/AC combiner	5		
Nr. of strings in one inverter	6		
Nr. of PV panels in one string	9		
Nr. of bypass diodes in one PV panel	3		
Whole PV plant specs	Nr of units		
Transformers	6		
Inverters	30		
PV panels	1620		
Based on the failure type fill in the following:	OK/failed	nr of units affected	percentage working
Grid connection	ok		0,999588477
Transformer/AC combiner	ok		0,999176955
Inverter failure	ok		0,997530864
Bypass diode(s) failure (accompanied by failure in PV panel)	ok		1
PV panel failure	ok		1
Bypass diode(s) turned on	failed	2	0,925925926

Figure 22. Illustration of exemplary park structure and failure.

At first the percentage of string output is calculated, this is done using equations (1) and (3) as follows:

$$F_{PV\ module} = \frac{N_{bypass\ diodes} - N_{activated}}{N_{bypass\ diodes}} = \frac{3-2}{3} = 0.3333 \tag{1}$$

$$F_{string} = \frac{(N_{modules}-1) + F_{PV\ module}}{N_{modules}} = \frac{(9-1)+0.33}{9} = 0.9259 \tag{3}$$

It should be noted that PV panel failure and bypass diode failure levels are not calculated since they are alternative failure modes to turned on bypass diodes. Only one failure of those three can exist at a time.

In order to determine the output from inverters, equation (6) is used as follows:

$$F_{inverters} = \frac{(N_{inverters}-1) + \frac{(N_{strings}-1)+F_{string}}{N_{strings}}}{N_{inverters}} = \frac{(5-1)+\frac{(6-1)+0.9259}{6}}{5} = 0.9975 \tag{6}$$

In order to determine the output from transformers, the same logic as in equation (3) is implemented:

$$F_{transformers} = \frac{(N_{transformers}-1) + F_{inverters}}{N_{transformers}} = \frac{(3-1)+0.9975}{3} = 0.99917 \tag{3}$$

Following the same logic, output from grid connection points is calculated as follows:

$$F_{grid} = \frac{(N_{grid}-1) + F_{transformers}}{N_{grid}} = \frac{(2-1)+0.99917}{2} = 0.99959 \tag{3}$$

56

Final factor (in this case 0.99959) is further implemented for calculation of production during the failure. It is done by multiplying it with hourly production for the whole year. Production losses are calculated by subtracting production during the failure from the estimated production. All calculations are done for each hour of the year.

4.3. Tool Outputs

Tool introduced in this project is Excel based table, that helps to estimate power losses due to component failures in PV plants. It aids with financial decisions based on maintenance/spare part cost and estimated production loss. Tool indicates more preferable solution based on the inserted data for two cases. In Figure 23 representation of two scenarios can be seen, failure period in first case is longer, but maintenance is 5000 € less expensive. The price marginal inserted corresponds to the renewable energy subsidy in Estonia for 2019 (Elering, 2019).

Price Marginal	53,7			
SCENARIO 1			SCENARIO 2	
Detection of failure	01-May		Detection of failure	01-May
Maintenance complete	20-May		Maintenance complete	10-May
Maintenance cost	15000		Maintenance cost	20000
Start row	2881		Start row	2881
End row	3337		End row	3097
Calculate energy losses			Calculate energy losses	
Lost Production [W]	116388226		Lost Production [W]	50548116
Lost Profit	11940		Lost Profit	4875
Sum cost	🔴 26940		Sum cost	🟢 24875

Figure 23. Tool presentation of calculated production losses data

As can be seen, production losses are higher due to the longer failure period in the first scenario. Red mark indicates that given solution is less beneficial for the company compared to the second scenario. This is due to the larger total expenses, that can be seen in the same cell with the red or green mark, which form from production losses

and maintenance cost needed to repair the failure. Inversely, green mark indicates that given scenario is more financially reasonable for the company. Therefore, it can be concluded that in given case more expensive maintenance benefits the company since it allows PV plant to become operational earlier. Further scenarios are analysed in chapter 5.2.

5. Case Study of the PV Park in Estonia

Case study is carried out to analyse production losses due to different failures. PV plants used in this work are located in Pärnu, Estonia (latitude 58.4069 and longitude 24.5264). At the time of writing this project given park complex is the largest photovoltaic park in Estonia.

Figure 24. Aerial photo showing the layout of the Pärnu Päikesepargid PV plants.

Source Google Earth Pro.

Projects and construction of the PV plants was ordered by Pärnu Päikesepargid companies, which are owned by AS Eesti Gaas (owning 80% stake) and Paikre OÜ (owning 20% stake). AS Eesti Gaas is one of the largest and most experienced energy companies in Estonia, with core product and competence in natural gas being the leading company in Baltic States, namely providing complete energy solutions based on natural gas, owning the largest network of compressed gas filling stations with optional biomethane, and as only company that has developed stable liquefied natural gas (LNG) supply and bunkering capability in the Baltic region (AS Eesti Gaas, 2019).

AS Eesti Gaas is also starting to grow its share of electricity production from photovoltaic solar plants. Paikre OÜ is company focusing on waste management in Pärnu, Estonia. Paikre OÜ managed the closure of Rääma landfill that was actively used from 1957 to 2006, during the closure activities heat and electricity cogeneration plant working on landfill gas was constructed and it started producing electricity in 2011 (Paikre OÜ, 2019). PV plant analysed in this work was constructed on the old closed landfill to use this land in a sustainable electricity generation purpose in addition to the landfill gas collection and usage. The PV plant complex consists of four equal solar parks, named Pärnu Päikesepark 1, 2, 3, and 4. PV plant complex specifics are given below.

	The PV plant complex
Type of PV panels used	Hyundai, 360 W (HiS-S360RI)
Number of PV panels mounted	12960
PV panel inclination	30°
Installed PV capacity	4.7 MW
Type of inverters used	ABB, 100 kW (PVI-100)
Number of inverters installed	10 in each park, 40 in total
Number of strings per inverter	18
Number of panels per string	18
Installed inverter capacity	4 MW

Table 8. Specifics of Pärnu Päikesepargid Complex.

5.1.   Models Created Using HelioScope

In order to carry out case study, parks had to be simulated using solar design software. Since the author was offered to use full licence of the HelioScope, the accuracy of the program was investigated. A third-party engineering company has confirmed that HelioScope and PVSyst products are within 1% at each step of calculation, using nearly all or the same equations for the calculation of energy yield (Folsolm Labs, 2019). A study carried out to estimate accuracy of the photovoltaic installations planning software found that PV*Sol and PVSyst display similar errors when calculating energy

yield (Axaopoulos, et al., 2014). Taking into account that PV*Sol trial version was alternative considered, it was evident that with similar accuracy full license software is preferred.

HelioScope was used for creating four models for simulating production of the PV plants. Each park has 10 inverters with 100 kW power, in total having 1 MW of output power, each. Since there are 4 parks, the total output power from the park complex is 4 MW.
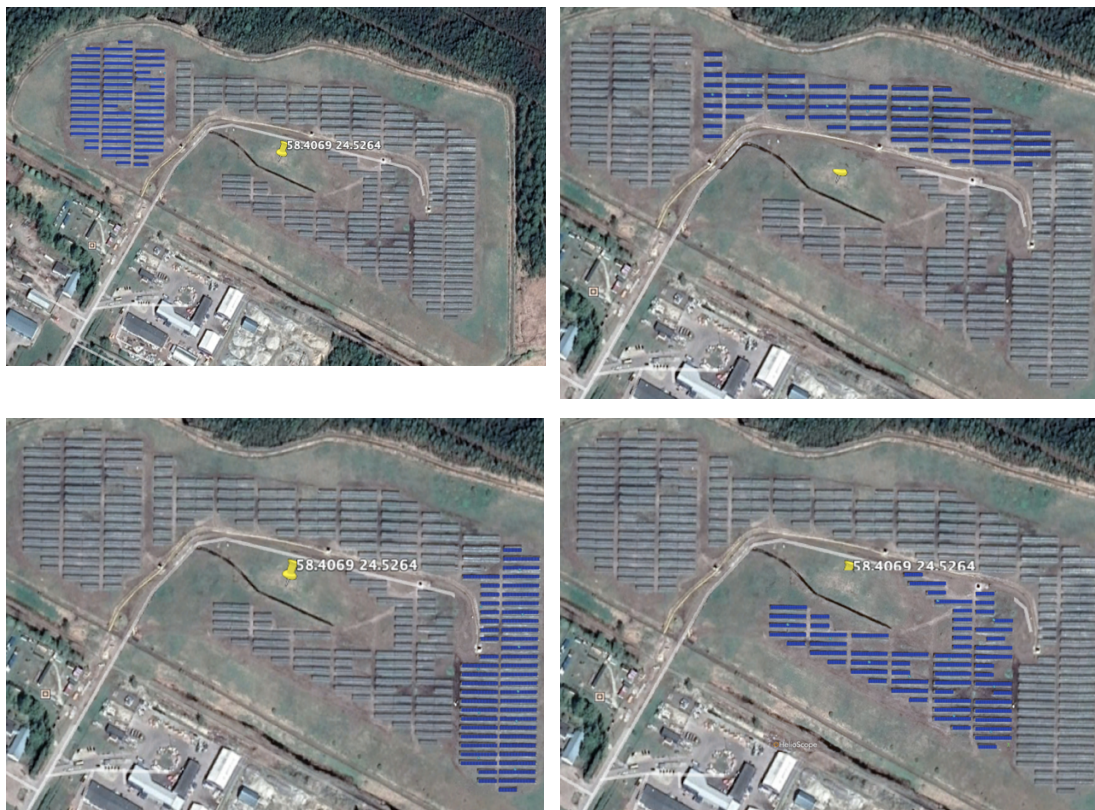
Figure 25. Layouts of PV parks from upper left to lower right showing Pärnu Päikesepark 1, 2, 3, and 4, respectively.

Models were created following the data provided by AS Eesti Gaas (PV modules, inverters, layout, panel inclination, rack distance etc.). Weather data used for the initial modelling was the satellite-based data from Meteonorm for the given coordinates. On the dust intensity map used in a study conducted by (Maghami, et al., 2016), Estonia is classified as a Zone 1, where dust conditions are 5.2-8.1 $\mu m/m^3$. On the same map Great Britain is classified as a Zone 2 with dust conditions 8.1-12 $\mu m/m^3$. Study carried out

by (Ghazi, et al., 2013) found that solar intensity due to the dust in the UK was reduced by 5%. Therefore, soiling conditions were set to 2% to represent dust conditions in Estonia. For the cell temperature calculation Sandia temperature model was used, which includes the exponential factor for wind, to account for the exponential wind influence, while Diffusion model includes components for constant and wind based temperature diffusion (Folsom Labs, 2019).

Energy yield estimations for all PV parks were relatively similar. Since models are later used, the average AC power (inverter output) is analysed. Average energy production per year was 1.1 GWh and all four parks had energy production that differed less than 1% from the average (minimum 0.13% and maximum 0.85%). Therefore, it was decided that one model is used for the further analyses, namely Pärnu Päikesepark 4 model, since it was closest to the average production.

5.2.   Scenarios Using the Tool

Three scenarios are used for the analysis, namely transformer, inverter and PV panel failure. All scenarios are run for the two periods, maximum production period May-June and minimum production period November-December. All relevant device prices are estimated, electricity price is hourly data from Nord Pool for the 2018, and it is assumed that park receives renewable energy subsidy 53.7 €/MWh (Elering, 2019). It is important to note that for analysis Pärnu Päikesepark 4 model is used.

Based on the PV plant layout fill in the following:	Nr of units
Nr. of grid connection	1
Nr. of transformers/AC combiners	1
Nr. of inverters connected to one transformer/AC combiner	10
Nr. of strings in one inverter	18
Nr. of PV panels in one string	18
Nr. of bypass diodes in one PV panel	3
Whole PV plant specs	Nr of units
Transformers	1
Inverters	10
PV panels	3240

Figure 26. Information about the Pärnu Päikesepark 4 devices and structure.

5.2.1.   Transformer Failure

Given scenario analyses situation where transformer has failed and therefore whole production is zero. It is estimated that 1MW step-up transformer replacement costs 20 000 €, including the price of device as well as installation works, and it is estimated to take 45 days. However, there is a company offering same device and service with additional cost but with faster repair time - 30 days. At first, given problem is run during May and June, which are months with highest estimated production based on the Helioscope model. Results are given in Figure 27.

SCENARIO 1			SCENARIO 2	
Detection of failure	01-May		Detection of failure	01-May
Maintenance complete	14-Jun		Maintenance complete	31-May
Maintenance cost	20000		Maintenance cost	23000
Start row	2881		Start row	2881
End row	3937		End row	3601
Calculate energy losses			**Calculate energy losses**	
Lost Production [W]	265572794		Lost Production [W]	179064824
Lost Profit	28188		Lost Profit	18560
Sum cost	🔴 48188		Sum cost	🟢 41560

Figure 27. Illustration showing different scenarios based on the transformer repair time and cost in May-June.

Green mark indicates that second scenario is financially more reasonable. On one hand two weeks longer repair time means around 9 600 € production losses, but on the other hand, two weeks faster repair only 3 000 € larger cost, company will save 6 600 € if scenario 2 is chosen. The same problem is run during months with the lowest estimated production, namely November and December. Results are given in Figure 28.

SCENARIO 1			SCENARIO 2	
Detection of failure	17-Nov		Detection of failure	01-Dec
Maintenance complete	31-Dec		Maintenance complete	31-Dec
Maintenance cost	20000		Maintenance cost	23000
Start row	7681		Start row	8017
End row	8737		End row	8737
Calculate energy losses			**Calculate energy losses**	
Lost Production [W]	8122190		Lost Production [W]	7245135
Lost Profit	919		Lost Profit	819
Sum cost	🟢 20919		Sum cost	🔴 23819

Figure 28. Illustration showing different scenarios based on the transformer repair time and cost in November-December.

As can be seen from the Figure 28, green mark indicates that first scenario is financially more reasonable. This is due to low production during the winter months. It can be seen that in both cases lost profit due to transformer failure is less than 1 000 €. Therefore, additional cost of 3 000 € is not justified. Company will save if they choose the first scenario.

5.2.2. Inverter Failure

Given scenario analyses situation where inverter has failed and therefore 1/10 of whole production is lost. ABB PVS 100 kW solar inverter costs 9 300 € (CCL Components Ltd, 2019). Estimated additional installation cost is 500 € and expected repairment period up to 3 weeks. However, another company has given inverter in storage near the site and is able to switch it with failed one in one week, for total price of 12 000 €. At first, given problem is run during May, which is month with the highest estimated production based on the Helioscope model. Results are given in Figure 29.

SCENARIO 1	
Detection of failure	01-May
Maintenance complete	21-May
Maintenance cost	9800
Start row	2881
End row	3361

Calculate energy losses

Lost Production [W]	12264482
Lost Profit	1245
Sum cost 🔴	11045

SCENARIO 2	
Detection of failure	01-May
Maintenance complete	07-May
Maintenance cost	10500
Start row	2881
End row	3025

Calculate energy losses

Lost Production [W]	2989654
Lost Profit	295
Sum cost 🟢	10795

Figure 29. Illustration showing different scenarios based on the inverter repair time

and cost in May.

As can be seen from the Figure 29, green value indicates that second scenario is financially more reasonable. Production losses are 76% higher during 3-week period compared to one week. Faster maintenance costs 700 € more compared to additional losses sustained during longer period worth 950 €. It can be concluded that more expensive but faster maintenance is preferred based on finances. The same problem is run during month with the lowest estimated production, namely December. Results are given in Figure 30.

SCENARIO 1	
Detection of failure	01-Dec
Maintenance complete	21-Dec
Maintenance cost	9800
Start row	8017
End row	8497

Calculate energy losses

Lost Production [W]	417225
Lost Profit	48
Sum cost 🟢	9848

SCENARIO 2	
Detection of failure	01-Dec
Maintenance complete	07-Dec
Maintenance cost	10500
Start row	8017
End row	8161

Calculate energy losses

Lost Production [W]	206982
Lost Profit	24
Sum cost 🔴	10524

Figure 30. Illustration showing different scenarios based on the inverter repair time

and cost in December.

As can be seen from the Figure 30, green value indicates that first scenario is financially more reasonable. Estimated production in December is low and therefore higher maintenance cost does not justify itself financially.

5.2.3.   PV Panel Failure

Given scenario analyses situation where PV panel has failed and it is accompanied by bypass diodes failure disabling electricity generation in one string. Here a different approach is implemented since PV panel failure means rather low losses compared to inverter and transformer failures. It is estimated that PV panel cost with transportation and installation is 150 €, however if PV panel replacement is done together with another maintenance activities, only panel cost of 90 € is needed. Subsequently, the period, where PV panel replacement can be postponed to be carried out when O&M crew is expected to visit the park, is studied. The main objective is to find during how long period around 60 € is lost due to the failure. If during this period there is another maintenance scheduled, it would be reasonable to combine those activities, otherwise, more expensive solution is preferred. Two periods are considered. This can be seen in Figure 31.

SCENARIO 1			SCENARIO 2	
Detection of failure	01-May		Detection of failure	01-Nov
Maintenance complete	19-May		Maintenance complete	12-Mar
Maintenance cost			Maintenance cost	
Start row	2881		Start row	7297
End row	3313		End row	1681
Calculate energy losses			**Calculate energy losses**	
Lost Production [W]	602477		Lost Production [W]	590442
Lost Profit	62		Lost Profit	61
Sum cost	🔴 62		Sum cost	🟢 61

Figure 31. Illustration showing length of the period during which around 60 € profit losses is generated starting from 1st of May and 1st of November.

Firstly, when the failure is detected on 1st of May, then by 19th of May a little over 60 € is lost due to failure. If during this period there is another maintenance event scheduled it is advised to carry out PV panel change during this event. If there are no events scheduled for this time period, separately ordered PV panel change can be beneficial. However, if the same failure is detected on the 1st of November, then the same amount (60 €) is lost by 12th of March. From 1st of November to 12th of March is almost 7 times longer period than from 1st of May to 19th of May. It is highly likely that during 132 days there will be a team sent to or scheduled to visit the solar park and therefore PV panel change can be carried out in addition to other works.

6. Discussion

Critical and self-reflective discussion is given regarding the development process and results obtained. Tool limitations are analysed and future work addressed.

6.1.   Discussion of Tool Development

Tool development was done based on the 5 principles displayed below:

1. Tool allows easy input regarding failure types;

2. Tool uses hourly production data for specified PV plant;

3. Tool conducts hourly calculations when considering monetary losses;

4. Tool takes into account failure time period and repairment cost;

5. Tool indicates favourable scenario based on the inserted data.

Regarding the developing environment in which the tool was built, Microsoft Excel was used to due to its wide usage in companies. Together with Excel, VBA was used for the purpose of automating tool's calculation of production losses during specified period.

In the process of developing the tool, Eesti Gaas was consulted in order to legitimize the approach taken for building the tool. Two in depth consultations were carried out, accompanied by site visit in June of the PV plant used in the case study and followed by frequent communication about proceedings of the tool development.

6.2.   Discussion of Results

In case study it was observed that the highest energy losses are due to the inverter and transformer failures. This is also stated by (Baschel, et al., 2018) when studying component reliability on large scale photovoltaic system performance, concluding that based on actual failure probabilities, inverter and transformer failures are the largest contributors to the production losses, even when their failure rates are low.

Results retrieved from the case study based on the data inserted are:

1. Higher maintenance cost but faster maintenance during high solar resource periods is more likely to be profitable than during low solar resource periods;

2. Maintenance period importance is more significant during high solar resource periods than during low solar resource periods;

3. Financial justification is dependent on all parameters and developed tool proves to be able to aid with related issues.

Based on the scenarios run during maximum and minimum production months, it can be said that financially optimum decision changes with observed time of the year. This is due to the changes in solar resource throughout the year. What is more, results are related to the price information used. Therefore, data regarding best knowledge has to be inserted to benefit from the tool. It can be observed that higher maintenance cost due to faster repairment proves itself to be justified during months with high solar resource. Another conclusion drawn from this can be that maintenance period is more significant factor during high solar resource periods. To conclude with, it can be said that all parameters contribute to the output of the tool and therefore given tool proves itself to be useful for estimating different outcomes with minimal effort.

On the contrary, it must be emphasised that given results are drawn from the specific case study, with estimated prices and production model compliant with specific layout for given large scale PV plant and weather data consistent with Estonian climate. For further conclusions given tool has to be implemented in real situations and in different PV parks.

6.3.   Tool Limitations

Developed tool has some limitations that have to be accounted for. Given tool is meant for symmetrical PV plants that have identical branches under every component, i.e. each string has the same number of PV panels, each maximum power point tracker has the same number of strings connected, each inverter has the same number of maximum power point trackers etc. Calculations inserted in Excel are meant for string inverters,

but the overall logic can be applied for the central inverter systems as well. It is assumed that person using the tool has access to modelling software and is able to carry out simulations to receive hourly production values and holds information about the detected failures to be able to fill in the table for production losses calculation. What is more, it is evident that the level of accuracy also depends on the PV plant model compiled by the user.

Another aspect of tool usage is that due to the large amount of data, namely yearly hourly data of 8760 rows, production loss calculations with VBA do take some time. Therefore, using the tool requires some patience, especially when there are several scenarios to consider. It still saves a significant amount of time compared to analysing production losses without given tool.

Developed tool is based on the normal year and in case of a leap year it must be noted that if the failure period includes the last day of February, production loss calculation does not take it into account. Easy solution is to add additional day to the failure period.

Given tool is designed to evaluate production loss from single failure type in one branch. However, there is a workaround to evaluate production losses that are from multiple sources. It requires the user to run both cases and on relevant device level take into account calculated losses. For instance, equation and explanation is given for the situation, where one inverter has substring failure due to panel failure followed by the bypass diodes failure and the second inverter has failed. Firstly, Figure 32 is given to illustrate the problem.
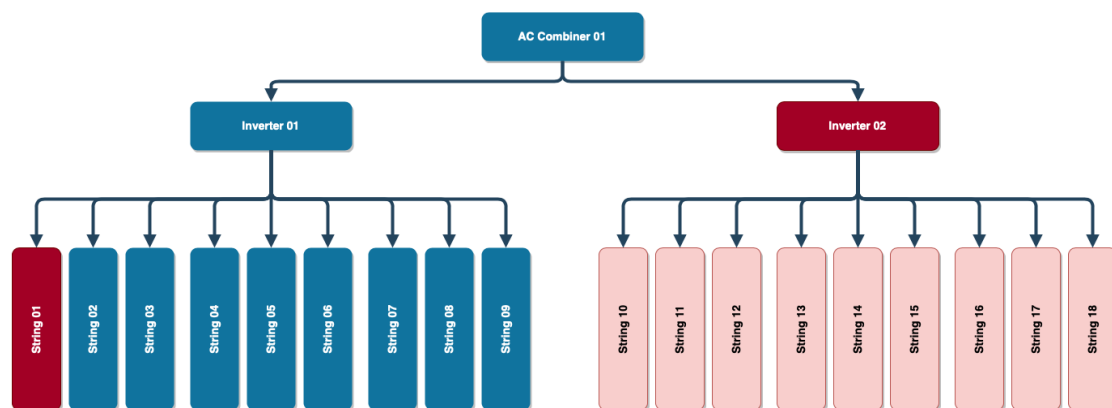
Figure 32. Illustration of the PV plant failures

Dark and light red represent the failure root and consequent power losses respectively. In case of an inverter failure power output is zero and all connected panels are not able to produce electricity. To calculate AC combiner factor of power output, both cases must be calculated in advance using the tool and then used in the inverters output formula

$$F_{inverters} = \frac{(N_{inverters} - N_{branches}) + F_{case1} + F_{case2}}{N_{inverters}} \qquad (7)$$

where,

$F_{inverters}$ = a total factor of output power from inverters;

F_{case1} = a factor of inverter output power in case 1, currently output when one string has failed;

F_{case2} = a factor of inverter output power in case 2, currently output when one inverter has failed;

$N_{inverters}$ = a number of inverters connected to AC combiner or transformer;

$N_{branches}$ = a number of inverter branches that have failures.

6.4.   Future Work

In order to receive more data about the accuracy of the developed tool, proposed future work includes further analysis regarding real production data. Since PV plant used in this work as a case study was connected to the grid in June 2019, and in first stages communication problems between data storage and inverters were apparent, there were not enough data to carry out extensive analysis. However, this can be examined when more data is available.

Furthermore, given tool is meant for evaluating PV plants with symmetrical structure. This means that each inverter has the same number of strings and each string has the same number of PV panels. While symmetrical parks are common when it comes to large scale parks, there are exceptions. In order to benefit from the tool with asymmetrical PV plant, further development is recommended. Overall logic does not have to be changed, however more specific data has to be inserted for the tool to be accurate. Figure 33 illustrates one way how additional data could be added.

INVERTER TYPE 1				In case of failure fill:	If 1 bypass diode ON	0,66	
Power					If 2 bypass diodes ON	0,33	
Nr of inverters	2				If whole panel out	0	
Nr of MPPTs	2						

MPPT 1				MPPT 2			
String nr	Panels in given string	Failure	5,94	String nr	Panels in given string	Failure	0
1	18		18,00	1			
2	18	0,33	5,94	2			
3	17	0,66	11,22	3			
4				4			
5				5			
6				6			

INVERTER TYPE 2							
Power							
Nr of inverters							
Nr of MPPTs							

String nr	Panels in given string	Failure		String nr	Panels in given string	Failure	
1				1			
2				2			
3				3			
4				4			
5				5			
6				6			

Figure 33. Illustration of possible layout for asymmetrical PV park data.

Tool extension has to be dynamic in order to allow different inverters with different number of maximum power point trackers and PV panel strings to be inserted. In case of asymmetrical park, inverter power information is also needed.

What is more, one of the possible extensions of this work could be the monitoring system for failure detection. This can be based on reverse logic implemented in this tool. However, in large scale parks detection of single panel failure (or even failure that triggers one bypass diode to turn on) is not accurate based on authors view and experiments carried out in the early stages of this dissertation. Regardless of that, detection of inverter or higher-level failures should be straightforward with access to measured weather data.

To finish with, the most valuable work might be done based on the feedback from the company Eesti Gaas AS after they have implemented given tool in different parks and have proposals for further improvements. Since it is meant to be easy to use, additional automation might be needed. For example, reading production data files from specified folder or using real-time price information.

7. Conclusions

Solar photovoltaic plants can be affected by several failure modes. Failures regarding photovoltaic panels degrade the modules power by obstructing solar resource to reach solar cell (e.g. encapsulant discolouration), by obstructing electricity path or intensifying leaks (e.g. corrosion of the cell metallisation), or by making module sensitive to accelerated degradation (e.g. delamination). Based on the literature review on different photovoltaic panel failures, most common interactions are mapped in Figure 5. When it comes to inverters and transformers, failures are discussed and found that influence on production is greater due to higher capacity. For instance, if inverter has failed, whole production originating from the inverter is lost, inversely, when one panel has failed, worst case scenario means that string production is lost. Failure detection, repair and prevention is done under operation and maintenance activities, which can be carried out by applying preventive, corrective, predictive, condition based and extraordinary maintenance. Field inspections to identify photovoltaic panel failures include infrared imaging, electroluminescence imaging and current-voltage curve tracking. Failures regarding inverters and transformers can be identified from production data and failure codes transmitted.

Developed Excel based tool consists of two main parts. Firstly, factor at which solar plant is working at after failure is determined. This is done by taking into account the structure of a plant and combining this information with occurring failure. Failure is inserted in the tool by defining the range of failure, it consists of bypass diode, photovoltaic panel, inverter, combiner/transformer and grid connection failure levels. Secondly, based on the estimated production data and failure period production losses are calculated by implementing created Visual Basic for Applications code. Created tool fulfils its purpose and is able to aid with calculation of production losses. Tool is uploaded on the University of Strathclyde Energy Systems Research Unit's Individual Theses website.

Created tool was used for analysing exemplary cases. Solar plant used in the case study is owned by Eesti Gaas AS and Paikre OÜ, and is as of now the largest solar park complex in Estonia. HelioScope model was created for 4 parts of the solar park complex

to receive hourly production estimations. Based on the analysis of given park and scenarios specified it can be concluded that maintenance period length imposes more significant influence during high solar resource periods than during low solar resource periods. Higher maintenance cost and faster maintenance proves to be more profitable during high solar resource periods. All in all, financial justification of preferred scenario is dependent on all parameters inserted and therefore accuracy of inserted information is vital.

To offer critical review of tool implementation, its limitations are pointed out. In order to receive accurate results and benefit from the tool those limitations have to be accounted for. Given tool is meant for usage in symmetrical plants for evaluating production losses from single failure type in one branch. However, there is a workaround introduced in chapter 6.3 for evaluating multiple failure types and possible tool layout for asymmetrical parks introduced in chapter 6.4. Tool usage requires access to the modelling software to create plant model and receive estimation for hourly production. It is common practice that in case of large scale photovoltaic panel parks given analysis are carried out in the planning stage and therefore given model can be easily updated and used in the tool. It should be noted that quality of the model also influences accuracy of the tool calculations. Due to the amount of data processed, calculations take some time depending on the computer's capability. However, if tool is implemented correctly taking into account all of the limitations, it aids with production losses evaluation.

Bibliography

Anon., 2013. *What happens when a solar panel fails?*. [Online]
Available at: http://greencarlisle.org/wordpress/wp-content/uploads/2013/06/What-Happens-When-a-Solar-Panel-Fails.pdf [Accessed 25 July 2019].

Anon., 2019. *The Electrochemical Society*. [Online]
Available at: https://www.electrochem.org/corrosion-science [Accessed 8 July 2019].

AS Eesti Gaas, 2019. *Eesti Gaas.* [Online]
Available at: https://www.gaas.ee/en/company/ [Accessed 20 July 2019].

Axaopoulos, P. J., Fylladitakis, E. D. & Gkarakis, K., 2014. Accuracy analysis of software for the estimation and planning of photovoltaic installations. *International Journal of Energy and Environmental Engineering,* 5(1), pp. 1-8.

Badiee, A., Ashcroft, I. & Wildman, R., 2016. The thermo-mechanical degradation of ethylene vinyl acetate used as a solar panel adhesive and encapsulant. *International Journal of Adhesion & Adhesives,* Volume 68, pp. 212-218.

Baschel, S., Koubli, E., Roy, J. & Gottschalg, R., 2018. Impact of Component Reliability on Large Scale Photovoltaic Systems' Performance. *Energies,* 11(6), p. 1579.

Bauer, J. Großer, S., Hagendorf, C., Schütze, M., Breitenstein, O., 2012. On the mechanism of potential-induced degradation in crystalline silicon solar cells. *Physica Status Solidi (RRL),* 6(8), p. 331 – 333.

British Standard, 2017. *BS EN13306:2017.* s.l.:British Standards Institution 2019 .

Brooks, A. E., Cormode, D., Cronin, A. D. & Kam-Lum, E., 2015. *PV system power loss and module damage due to partial shade and bypass diode failure depend on cell behavior in reverse bias.* New Orleans, LA, USA, IEEE 42nd Photovoltaic Specialist Conference (PVSC).

C Gascoigne Ltd. , 2019. *Solar Inverter Faults.* [Online]
Available at: http://www.cgascoigne.co.uk/services/solar-panel-maintenance-repairs/solar-inverter-repairs/solar-inverter-faults/ [Accessed 2 August 2019].

CCL Components Ltd, 2019. *ABB PVS 100kW Solar Inverter with SX Wiring Box - Three Phase - 6 MPPT.* [Online]
Available at: https://www.cclcomponents.com/abb-pvs-100kw-solar-inverter-with-sx-wiring-box-three-phase-6-mppt?gclid=CjwKCAjw7anqBRALEiwAgvGgm6e7RBuOFl6nFMGszhHWyWW199RIzP1rhikXaau6fLiVQpfQcD8tLhoCIDEQAvD_BwE [Accessed 7 August 2019].

Celik, Ö., Teke, A. & Tan, A., 2018. Overview of micro-inverters as a challenging technology in photovoltaic applications. *Renewable and Sustainable Energy Reviews,* Volume 82, pp. 3191-3206.

Dolara, A., Lazaroiu, G. C., Leva, S., Manzolini, G., Votta, L., 2016. Snail Trails and Cell Microcrack Impact on PV Module Maximum Power and Energy Production. *IEEE Journal of Photovoltaics,* 6(5), pp. 1269 - 1277.

Duerr, I., Bierbaum, J., Metzger, J., Richter, J., Philipp, D., 2016. Silver grid finger corrosion on snail track affected PV modules-investigation on degradation products and mechanisms. *Energy Procedia,* Volume 98, pp. 74-85.

Elering, 2019. *Eesti Vabariigi juubeliaasta tõi juurde 100 megavatti päikeseelektrijaamu.* [Online]
Available at: https://elering.ee/eesti-vabariigi-juubeliaasta-toi-juurde-100-megavatti-paikeseelektrijaamu [Accessed 1 August 2019].

Elering, 2019. *Taastuvenergia toetus.* [Online]
Available at: https://elering.ee/taastuvenergia-toetus [Accessed 7 August 2019].

Enbar, N., Weng, D. & Klise, G., 2015. *Budgeting for Solar PV Plant Operations & Maintenance: Practices and Pricing,* California: Electric Power Research Institute.
Erath, D., 2009. *Printing Techniques in the c-Si PV Industry – a Brief Technological Overview.* [Online]
Available at:
https://www.internationalcircle.net/international_circle/circular/issues/10_01/ICJ_03_08_erath.pdf [Accessed 1 July 2019].

Folsolm Labs, 2019. *HelioScope vs. PVsyst.* [Online]
Available at: https://help.helioscope.com/article/52-helioscope-vs-pvsyst [Accessed 20 July 2019].

Folsom Labs, 2019. *HelioScope: Mathematical Formulation.* [Online]
Available at: https://www.helioscope.com/documentation/mathematical-formulation [Accessed 21 July 2019].

Formica, T. J., Khan, H. A. & Pecht, M. G., 2017. The Effect of Inverter Failures on the Return on Investment of Solar Photovoltaic Systems. *IEEE Access,* Volume 5, pp. 21336 - 21343.

Gade, V., Shiradkar, N., Paggi, M. & Opalewski, J., 2015. *Predicting the Long Term Power Loss from Cell Cracks in PV Modules.* New Orleans, LA, USA, IEEE 42nd Photovoltaic Specialist Conference (PVSC).

Ghazi, S., Ip, K. & Sayigh, A., 2013. Preliminary Study of Environmental Solid Particles on Solar Flat Surfaces in the UK. *Energy Procedia,* Volume 43, pp. 765-774.

Honsberg, C. & Bowden, S., 2019. *PVEducation.* [Online]
Available at: https://www.pveducation.org [Accessed 25 June 2019].

Jahn, U., Herz, M., Köntges, M., Parlevliet, D., Paggi, M., Tsanakas, I., Stein, J. S., Berger, K. A., Ranta, S., French, R. H., Richter, M., Tanahashi, T., 2018. *Review on Infrared and Electroluminescence Imaging for PV Field Applications.* s.l., International Energy Agency Photovoltaic Power Systems Programme.

Jan, S. T., Afzal, R. & Khan, A. Z., 2015. *Transformer Failures, Causes & Impacts.* Bali, International Conference Data Mining, Civil and Mechanical Engineering.

Köntges, M., Kurtz, S., Packard, C., Jahn, U., Berger, K. A., Kato, K., Friesen, T., Liu, H., Van Iseghem, M., 2014. *Review of Failures of Photovoltaic Modules,* s.l.: International Energy Agency Photovoltaic Power Systems Programme.

Kaplani, E., 2012. Degradation Effects in sc-Si PV Modules Subjected to Natural and Induced Ageing after Several Years of Field Operation. *Journal of Engineering Science and Technology Review,* 5(4), pp. 18-23.

Klimaraad, 2018. *PV-module-with-three-bypass-diodes-dividing-the-panel-into-three-strings-A-large-maple.* [Online]
Available at: https://www.klimaraad.nl/info-zonne-energie/zonnepanelen/techniek-zonnepanelen/attachment/pv-module-with-three-bypass-diodes-dividing-the-panel-into-three-strings-a-large-maple [Accessed 15 August 2019].

Lausch, D., Naumann, V., Graff, A., Hähnel, A., Breitenstein, O., Hagendorf, C., Bagdahn, J., 2014. Sodium Outdiffusion from Stacking Faults as Root Cause for the Recovery Process of Potential-induced Degradation (PID). *Energy Procedia,* Volume 44, pp. 486-493.

Luo, W., Khoo, Y. S., Hacke, P., Naumann, V., Lausch, D., Harvey, S. P., Singh, J. P., Chai, J., Wang, Y., Aberle, A. G., Ramakrishna, S., 2017. Potential-induced degradation in photovoltaic modules: a critical review. *Energy & Environmental Science,* 10(1), pp. 43-68.

M.A.Munoz, M.C.Alonso-García, NievesVela & F.Chenlo, 2011. Early degradation of silicon PV modules and guaranty conditions. *Solar Energy,* 85(9), pp. 2264-2274.

Maghami, M. R., Hizam, H., Gomes, C., Radzi, M. A., Rezadad, M. I., Hajighorbani, S., 2016. Power loss due to soiling on solar panel: A review. *Renewable and Sustainable Energy Reviews,* Volume 59, pp. 1307-1316.

Molenbroek, E., Waddington, D. & Emery, K., 1991. *Hot spot susceptibility and testing of PV modules.* Las Vegas, Conference Record of the 22th IEEE.

Ogbomo, O. O., Amalu, E. H., Ekere, N. N. & Olagbegi, P. O., 2017. A review of photovoltaic module technologies for increased performance in tropical climate. *Renewable and Sustainable Energy Reviews,* Volume 75, pp. 1225-1238.

Omazic, A., Oreski, G., Halwachs, M., Eder, G. C., Hirschl, C., Neumaier, L., Pinter, G., Erceg, M., 2019. Relation between degradation of polymeric components in crystalline silicon PV module and climatic conditions: A literature review. *Solar Energy Materials and Solar Cells,* Volume 192, pp. 123-133.

Paikre OÜ, 2019. *Paikre OÜ.* [Online]
Available at: https://paikre.ee/ettevottest/ [Accessed 20 July 2019].

Petrova, V., 2019. *Estonia powers up 100 MW of solar parks in 2018.* [Online]
Available at: https://renewablesnow.com/news/estonia-powers-up-100-mw-of-solar-parks-in-2018-640078/ [Accessed 1 August 2019].

Pingel, S., Frank, O., Winkler, M., Daryan, S., Geipel, T., Hoehne, H., Berghold, J., 2010. *Potential Induced Degradation of Solar Cells and Panels.* Berlin, Germany, IEEE Photovoltaic Specialists Conference.

Power From Sunlight, 2017. *Solar Bypass Diode Guide: This Is What You Should Know About Solar Bypass Diodes.* [Online]
Available at: https://www.powerfromsunlight.com/solar-bypass-diode-guide-this-is-what-you-should-know-about-solar-bypass-diodes/ [Accessed 15 August 2019].

Power From Sunlight, 2017. *What You Need To Know About Solar Panel Junction Box.* [Online]
Available at: https://www.powerfromsunlight.com/what-you-need-to-know-about-solar-panel-junction-box/ [Accessed 15 August 2019].

Revie, R. W. & Uhlig, H. H., 2008. In: 4. Edition, ed. *Corrosion and Corrosion Control: An Introduction to Corrosion Science and Engineering.* New Jersey: John Wiley & Sons, Inc., p. 1.

Scholten, D. M., Ertugrul, N. & Soong, W. L., 2013. *Micro-Inverters in Small Scale PV Systems: A Review and Future Directions.* Adelaide, Australian Universities Power Engineering Conference.

Shapley, 2011. *Semiconductors and Silicon Solar Cells.* [Online]
Available at: http://butane.chem.uiuc.edu/pshapley/Environmental/L9/2.html [Accessed 15 August 2019].

Shin, W. G., Ko, S. W., Song, H. J., Ju, Y.C., Hwang, H. M., Kang, G. H., 2018. Origin of Bypass Diode Fault in c-Si Photovoltaic Modules: Leakage Current under High Surrounding Temperature. *Energies,* 11(9).

Solar DAO, 2017. *Everything You Need to Know About Operations & Maintenance (O&M) For Utility Scale PV Solar Plants.* [Online]
Available at: https://medium.com/@solar.dao/everything-you-need-to-know-about-operations-maintenance-o-m-for-utility-scale-pv-solar-plants-9d0048e9b9a2 [Accessed 17 July 2019].

SolarPower Europe O&M Task Force, 2018. *Operation & Maintenance Best Practices Guidelines / Version 3.0,* Brussels: SolarPower Europe O&M Task Force.

Tariq, M. S., Butt, S. A. & Khan, H. A., 2018. Impact of module and inverter failures on the performance of central-, string- and micro-inverter PV systems. *Microelectronics Reliability,* Volume 88-90, pp. 1042-1046.

Viridian Concepts Ltd., 2017. *Solar PV Panels.* [Online]
Available at: http://www.viridiansolar.co.uk/resources-4-3-PV-solar-modules.html [Accessed 15 August 2019].

Wohlgemuth, J., Silverman, T., Miller, D. C., McNutt, P., Kempe, M., Deceglie, M., 2015. *Evaluation of PV Module Field Performance.* Golden, Colorado, National Renewable Energy Laboratory.

Zarmai, M. T., Ekere, N. N., Oduoza, C. F. & Amalu, E. H., 2015. A review of interconnection technologies for improved crystalline silicon solar cell photovoltaic module assembly. *Applied Energy,* Volume 154, pp. 173-182.

Appendix I

Supplementary Data File

Description:

The accompanying Excel macro-enabled workbook is the tool developed in this thesis. It aids with production losses calculation based on the estimated production and identified failure. What is more, in case of competitive maintenance offers, it indicates financially preferred one, based on the maintenance length and cost.

Filename:

EJR_lossescalc.xlsm